12-11-2017

THE LEFT HEMISPHERE'S STRUCTURAL CONNECTIVITY FOR THE INFERIOR FRONTAL GYRUS, STRIATUM, AND THALAMUS, AND INTRA-THALAMIC TOPOGRAPHY

Simone R. Roberts

THE LEFT HEMISPHERE'S STRUCTURAL CONNECTIVITY FOR THE INFERIOR FRONTAL GYRUS, STRIATUM, AND THALAMUS, AND INTRA-THALAMIC TOPOGRAPHY

by

SIMONE RENÉE ROBERTS

Under the Direction of Bruce Crosson, PhD

ABSTRACT

The neuroanatomy of language cognition has an extensive history of scientific interest and inquiry. Over a century of behavioral lesion studies and decades of functional neuroimaging research have established the left hemisphere's inferior frontal gyrus (IFG) as a critical region for speech and language processing. This region's subcortical projections are thought to be instrumental for supporting and integrating the cognitive functions of the language network. However, only a subset of these projections have been shown to exist in humans, and structural evidence of pars orbitalis' subcortical circuitry has been limited to non-human primates. This thesis demonstrates direct, intra-structural connectivity of each of the left IFG's gyral regions with the thalamus and the putamen in humans, using high-angular, deterministic tractography. Novel processing and analysis methods elucidated evidence of predominantly segregated cortical circuits within the thalamus, and suggested the presence of parallel circuits for motor/language integration along the length of the putamen.

INDEX WORDS: Tractography, Language, Inferior frontal gyrus, Pars orbitalis, Thalamus, Striatum

THE LEFT HEMISPHERE'S STRUCTURAL CONNECTIVITY FOR THE INFERIOR FRONTAL GYRUS, STRIATUM, AND THALAMUS, AND INTRA-THALAMIC TOPOGRAPHY

by

SIMONE RENÉE ROBERTS

A Thesis Submitted in Partial Fulfillment of the Requirements for the Degree of

Master of Science

in the College of Arts and Sciences

Georgia State University

2017

THE LEFT HEMISPHERE'S STRUCTURAL CONNECTIVITY FOR THE INFERIOR FRONTAL GYRUS, STRIATUM, AND THALAMUS, AND INTRA-THALAMIC TOPOGRAPHY

by

SIMONE RENÉE ROBERTS

Committee Chair: Bruce Crosson

Committee: Anastasia Bohsali

Tricia King

Electronic Version Approved:

Office of Graduate Studies

College of Arts and Sciences

Georgia State University

December 2017

DEDICATION

This Master's thesis is dedicated to

Beca Emma Gooch and Richard Cully Millhouse III.

- por aeternum, el alma se mueve -

ACKNOWLEDGEMENTS

This Master's thesis is a manifestation of the work, support, and inspiration of many, including my committee, my research labs at Georgia State University, Emory University, and the Center for Visual and Neurocognitive Rehabilitation at the US Department of Veterans Affairs, and others. Prior to commencement of my graduate studies, Anastasia Ford-Bohsali generously offered her time to teach me how to process DWI images. In addition to providing feedback as a member of my committee, Dr. Ford-Bohsali was instrumental in mentoring me as I learned to process tractography independently. Thomas Mareci's mentorship and collaboration was invaluable, and inspired me to learn more about the mathematics and computer science of streamline tractography. At the outset of my methodological ambitions, Stephen Towler taught me how to work efficiently in a Unix neuroimaging environment, including teaching me foundational Bash syntax and guiding novel code conceptualization. I pushed my lab's computing infrastructure to its limits repeatedly while developing methods and generally working on this thesis, and am grateful to Keith McGregor for his patience while assisting me with countless related obstacles. Steven Hirschmann applied his creativity and expertise in computer science to decipher and remedy a particularly perplexing C code bug. Lisa and Venkatagiri Krishnamurthy helped me develop reliable co-registration and subcortical segmentation pipelines. Stella Maria Tran and Jonathan Drucker made considerable contributions of time and effort by manually tracing each cortical ROI and scrutinizing sulcal boundaries with me until inter-rater reliability and consensus was achieved for every cortical ROI mask. Tricia King's insight as both my professor and committee member guided my framework for understanding and describing the importance of anatomical inquiry as behaviorally relevant in the field of neuropsychology. I am appreciative of Jessica Turner for her ongoing support of this thesis and my training during my transition into a research-centered degree concentration. It almost goes without saying that the previous research of my graduate advisor, Bruce Crosson, was pivotal to the inspiration and development of this thesis. Nonetheless, I am the most grateful for his mentorship and understanding, as without it this thesis and my academic journey would not have been possible. Finally and importantly, I'd like to thank my mom for a lifetime of unconditional love and support.

TABLE OF CONTENTS

LIST OF TABLES

LIST OF FIGURES

1 INTRODUCTION

Every cognitive or behavioral theory of brain function relies on the assumption of neuroanatomical plausibility. This assumption is not unique to the pursuits of neuroanatomists, neuroscientists, and neuropsychologists, but arguably an underlying truth pervasive throughout all scientific fields which endeavor to describe the behavior of individuals. Prior to the advent of neuroimaging, the pursuit of anatomical knowledge relied primarily on studies of non-human species and post-mortem autopsies. The ability to study the human brain *in vivo* with magnetic resonance imaging (MRI) has cleared the way for scientists to gather data and make inferences directly and noninvasively. With functional and structural MRI, scientists can infer which anatomical regions are recruited during specific behaviors and cognitive processes, observe patterns of regions that are recruited concomitantly, and deduce the white matter connectivity between these regions.

Functional MRI (fMRI) relies on changes in cerebral blood flow and blood oxygenation to produce blood-oxygen-level dependent (BOLD) contrast between mental states and/or while performing tasks. Observation of a statistically significant, positive BOLD signal change implies recruitment of a brain region during the task or mental state. Functional connectivity is inferred when the hemodynamic signature of BOLD signals correlate temporally across multiple regions. The ability to discern functional connectivity networks makes fMRI a powerful and invaluable tool in the behavioral and cognitive sciences, however it is not without limitations. Although fMRI is able to indicate which regions of the brain are behaviorally relevant during a task or state, it is not able to tell us why or how. Functional activation cannot be assumed to prove that a region performs or enables a behavior, as it is also possible for a region to show functional activation yet inhibit or interfere with processes supported by other brain regions. Further, fMRI does not explain how it is anatomically possible for regions within a functional network to communicate. Functional networks often consist of regions with only indirect means of communication, which may implicate additional grey matter structures and multi-synaptic white matter pathways. Hence, measures of structural connectivity are a necessary compliment to fMRI research.

Structural neuroimaging methods rely on diffusion-weighted MRI (DWI) to infer structural connectivity. DWI methods assess the rate and directionality of water diffusion for tractography and/or quantification of microstructural properties of cerebral white matter. Because microstructural metrics are scalars derived from the properties of water diffusion along multiple orientations, they are prone to inflation or deflation in complex regions and may not accurately represent crossing and/or branching fibers, especially when scalars are derived from non-isotropic voxels (Crosson et al., 2013; Oouchi et al., 2007). When considered carefully according to the surrounding anatomy, microstructural metrics can be useful for comparing white matter amongst cohorts. Microstructural metrics do not, however, independently provide information about structural connectivity to fill in the gaps that functional connectivity analyses fail to address. To determine structural connectivity, a visual map of inferred bundles of neuronal axons can be generated with white matter tractography. With deterministic tractography, a streamline is generated if water appears to diffuse anisotropically along a continuous and physically reasonable set of points. Irrelevant streamlines can then be filtered out with network tractography tools, such as those utilized for this thesis, leaving only the subsets of streamlines that directly connect two or more regions.

At surface level, streamline tractography only provides very specific anatomical data. But more broadly, tractography enables investigation of potential anatomical bases for functional connectivity. White matter pathways both support and constrain behavior, thus tractography enables inference regarding ways that distinct regions within functional networks might feasibly influence one another. This concept is critical clinically as structure is vulnerable to the effects of aging and/or pathology, and structural connectivity interruptions can lead to observable changes in behavior. Thus, white matter tractography is a relevant and valuable tool for understanding human behavior, including behavioral changes due to brain injury or disease.

1.1 Research Concept

The present study investigated cortico-striatal and cortico-thalamic/thalamo-cortical structural connectivities of the inferior frontal gyrus (IFG) potentially involved in language processing in healthy,

young adults. Well over a century has passed since Paul Broca first examined the brain of an aphasic man post-mortem and identified the IFG as a critical region of the brain for fluent speech output (1861b). Since this seminal discovery, scientists have empirically validated this claim *in vivo* using methods such as fMRI and transcranial magnetic stimulation (TMS) with both aphasic patients and healthy human subjects, and many of the IFG's structural connections have been established (see Sections 2 & 3). However, the subcortical circuitry for the IFG has only been described for 2/3 of the IFG's gyral regions, specifically pars triangularis (PTr) and pars opercularis (POp). Subcortical projections of the IFG's anterior/inferior-most region, pars orbitalis (POr), have not yet been substantiated in humans although research suggests the entire IFG has language-relevant subcortical connectivity (see Sections 2 & 3).

The lack of established, neuroanatomical knowledge describing POr's subcortical circuitry is of great concern given POr's relevance to verbal cognition and the widespread assumption that every frontal structure has subcortical connectivity, topics which will be addressed further in the sections to follow. Functional, behavioral evidence as well as present knowledge of cortico-cortical structural connectivity for the POr region is thus limited in application, and will remain so unless the neuroanatomical substrates of POr are substantiated empirically in healthy populations. Piecing together the topographical features of known white matter networks is also of consequence for applying anatomical knowledge to the sequelae of brain damage. Studying and treating patients with aphasia requires detailed knowledge of baseline assumptions. Subcortical aphasia syndromes resulting from infarct to the thalamus are well established and documented, and existing behavioral evidence (e.g. anomia subsequent to thalamic stroke) is sufficient to implicate the thalamus as a key player in the language network (see Sections 2.2.3 & 3.1). This evidence falls short, however, of describing exactly which frontal circuits must be interrupted to produce the deficits characteristic of thalamic aphasia, or which circuits could feasibly be recruited to promote recovery of language function. Detailed description of the intra-thalamic topography of cortico-thalamic/thalamo-cortical circuits in humans is requisite for addressing these inquiries.

To address the described gaps in scientific knowledge of human cortico-subcortical neuroanatomy, we used deterministic, white matter tractography for investigating potential direct

structural connections between POr and the neostriatum and between POr and the thalamus. In addition, we proposed that intra-thalamic, topographical relationships of IFG white matter networks could be evaluated and quantified from structural connectivity data produced by using an innovative tractography method that enables high-specificity estimation of white matter networks both between and within regions of interest.

2 LANGUAGE AND THE BRAIN

2.1 The Inferior Frontal Gyrus

Since Paul Broca first elevated the IFG to a position of eminence within the language domain, this frontal gyrus' functions have been dissected from many theoretical orientations through countless investigations and a wide array of methodological approaches. To this day, however, consensus about localization and distribution of specific cognitive functions within the IFG has not been satisfactorily attained. Some contemporary theorists argue against any clear dissociation of function or propose that the IFG plays only a broadly defined role in language processing, while others assert that distinctions observed in the functional neuroimaging literature are confounded by imprecise research paradigms (reviewed by Rodd, Vitello, Woollams, & Adank, 2015). Many prominent, competing models assume overlapping functional gradients across cortical regions (Dominey, Inui, & Hoen, 2009; Hagoort, 2014; Hagoort & Indefrey, 2014; Turken & Dronkers, 2011). Some also give consideration to the mismatch between visible, gyral regions studied by fMRI and underlying cytoarchitectonic features that may or may not delineate the borders of functional regions (Amunts & Zilles, 2015; Hagoort, 2005). Most researchers, however, agree that language processing is not randomly distributed across IFG cortices, but rather follows a general spatial, functional gradient. For instance, according to Hagoort and colleagues, spatial activation gradients of the IFG appear to reflect a semantic distribution across POr and PTr, a syntactic distribution across PTr and POp, and a phonological distribution across POp and the ventral premotor cortex.

It is of note that Hagoort and colleagues' models extend past the region widely known as "Broca's area". Broca's area consists of PTr and POp in the left hemisphere, representing only a subset of the IFG as the language eloquent cortex. This classical view of Broca's area is a historical misnomer that originated subsequent to Paul Broca's work naming the IFG in its entirety as the likely "seat of the faculty of articulate language" (1861a, 1861b, 1865). As a result, POr has become a lesser studied and consequently lesser understood region, in comparison with PTr and POp. To illuminate and combat the imbalanced popularity of Broca's area in scientific inquiry, Hagoort proposed a designation of "Broca's Complex" or "Broca's Region" that encapsulates Broca's initial contributions (POr, PTr, and POp) along with adjacent cortical regions of the language network (Hagoort, 2005).

2.1.1 Structural Evidence

Although to our knowledge POr's subcortical projections have never been scrutinized, existing evidence of Broca's area's capsular circuitry provides a compelling foundation for the study of the IFG's relationships with the subcortical brain. Ford, Triplett, et al., (2013) traced white matter streamlines of PTr and POp with deterministic tractography and found that cortical fibers from these regions lie within the internal capsule and converge in both the ventral anterior nucleus of the thalamus and the anterior-superior portion of the putamen. Direct projections to the caudate nucleus were not revealed by this research, although pathways approaching the surface of this structure were noted. However, it is widely agreed upon that the caudate nucleus has prominent frontal projections (Draganski et al., 2008; Verstynen, Badre, Jarbo, & Schneider, 2012), and evidence of direct connectivity has been reported by other research groups (Kotz, Anwander, Axer, & Knösche, 2013; Lehéricy et al., 2004; Mandelli et al., 2014). Notably, Lehéricy and colleagues used Basser, Mattiello, and LeBihan's (1994) pioneering, deterministic framework to produce fibers that link the head of the caudate nucleus to PTr and possibly POr. Ford et al.'s null findings may exemplify the difficulty of tracing direct structural connectivity for the caudate nucleus, or conversely might reflect a methodological limitation not yet addressed by software used for contemporary, high resolution diffusion tractography. Further investigation of these

cortico-striatal networks is necessary for more conclusive substantiation of the IFG's structural connectivity with the caudate nucleus.

Bohsali et al. (2015) later expanded upon their thalamic findings (Ford, Triplett, et al., 2013), demonstrating that classical Broca's area has structural connectivity with both the ventral anterior nucleus and the pulvinar nucleus of the thalamus. A portion of the observed structural connectivity passed through the ventral anterior nucleus and traversed the length of the thalamus via what appeared to be the white matter of the internal medullary lamina, ultimately reaching the pulvinar at the posterior end of the thalamus. Fronto-pulvinar connectivity is a critical finding as the pulvinar is believed to have reciprocal connectivity with many parietal, temporal, and occipital regions involved in other cognitive processes that support language, including hearing and vision (see Section 2.2). Thus, Bohsali et al.'s findings may describe the location of a possible mechanism for thalamic coordination amongst the cerebral lobes, as expounded upon by Crosson (2013) in his theory of thalamic function (see Section 2.2.3). Nishio et al. (2014) published evidence of similar findings from a probabilistic diffusion investigation of stroke patients during the first month following anterior thalamic infarct recovery. As described by the authors, the circuitry depicted by Supplementary Figure 4 appears to follow from the site of thalamic damage at the anterior nucleus, through the internal medullary lamina and the mediodorsal nucleus, to reach the temporopulvinar bundle of Arnold.

Presumably, POr may interact with PTr and POp indirectly for integrative linguistic processing by recruiting support from the thalamus and basal ganglia, although this has yet to be demonstrated as anatomically plausible. In contrast, direct cortico-cortical transmission has been explored and described by Lemaire et al. (2012). Lemaire and colleagues' research produced evidence of discernable, U-shaped fiber bundles connecting POr with PTr. In addition to basic anatomical virtue, Lemaire et al.'s findings are harmonious with behavioral evidence underlying Hagoort's delineation of a spatial gradient of semantic processing spanning POr and PTr in the left hemisphere's IFG.

2.1.2 Functional Evidence and Theory

Hagoort and Indefry (2014) explored the functional distribution of language in an fMRI meta-analysis focused on distinguishing the gradients of semantic and syntactic processing. Regions in the left temporal lobe, left medial prefrontal cortex, and right IFG variably presented as parts of the semantic and syntactic networks beyond the present discussion. Comprehension itself was reported to activate POr and PTr, in addition to the middle and superior temporal gyri.

Language tasks involving manipulation of semantic processing burden, semantically complex sentences, and semantic violations appeared to most reliably activate POr and PTr of the left hemisphere, indicating a semantic functional gradient across these regions (Hagoort & Indefry, 2014). Activation was also found in POp for semantic manipulation and violation studies, albeit at a much lesser frequency. These findings are consistent with the general consensus that POr and PTr play a strong role in semantic processing. Semantic judgment tasks administered outside of an MRI scanner, with and without TMS, have similarly indicated that semantic processing is likely associated with POr and PTr (Devlin, Matthews, & Rushworth, 2003; Gough, Nobre, & Devlin, 2005).

Discussion of the IFG's contribution to syntactic processing also resonates within the scientific community, although not without controversy. In Hagoort and Indefry's meta-analysis (2014), syntactic violations and manipulations typically activated the left hemisphere's PTr and POp. Similarly, studies with syntactically complex sentences tended to activate POp. Other authors have noted more extensive networks of activation in the IFG. Teichman et al. (2015) analyzed both healthy participants and subjects with frontal/striatal damage. Voxel-based lesion symptom mapping (VLSM) results indicated significant involvement of POr, PTr, and POp, in combination with the head of the caudate nucleus, for "phrasal syntax of noncanonical sentences and the morphosyntax of inflectional subregularities". Teichman et al.'s findings were specific to the caudate nucleus and did not extend to cortico-putaminal circuits upon analysis. Kotz, Frisch, von Cramon, and Friederici (2003) produced similar evidence of a cortico-striatal syntactic network with their event-related potential (ERP) lesion research that considered the basal ganglia as a whole.

Teichman and colleagues' (2015) findings are generally consistent with the theories put forth by Dominey et al. (2009) and Hinaut and Dominey (2013) regarding the syntactic contributions of IFG-striatal structural connectivity. Dominey and colleagues' theories extend beyond syntactic theory and are particularly descriptive of their conceptualization of POr's function, in combination with classical Broca's area and the subcortical brain. In these authors' model, cortico-striatal and cortico-thalamic/thalamo-cortical connectivity of the IFG are relied upon for lexico-semantic processing and syntactic unification. Broadly, POr is posited to play a modulatory and arguably executive role in verbal processing, maintaining structural cues from closed-class words for ongoing sentence context. Context encoded in POr influences information held in semantic working memory by POr and PTr, which in turn binds and integrates with thematic role information processed by POp and the ventral premotor cortex. This allows for real-time, word-level and sentence-level processing that takes into account the entire sentence. Anatomically, this modulation is enabled by overlapping, afferent projections from the IFG to the caudate nucleus of the basal ganglia. As noted in previous sections, current tractography evidence of this circuitry is not conclusive, although it is widely assumed to exist. Input to the caudate nucleus ultimately acts upon the thalamus, via one of the subcortical loops described in the following section. The thalamus' reciprocal connectivity with the cortex then synchronizes relevant cortical activation patterns. As mentioned above, Ford, Triplett, et al. (2013) demonstrated the existence of these circuits for classical Broca's area. The required structural connectivity for a POr-driven modulatory function has yet to be demonstrated, but might provide a reasonable means for the thalamus to orchestrate activation and integration amongst all three IFG regions.

Dominey and colleagues' model (Dominey et al., 2009; Hinaut & Dominey, 2013) also proposed that the mechanism that allows for lexico-semantic and syntactic unification promotes learning via cortico-striatal synaptogenesis at points of terminal overlap in the caudate nucleus. Inputs from POr, PTr, and POp would become strengthened in an associative memory network that permits future re-activation and generalization to new sentences adhering to learned grammatical structure. Ultimately, direct cortico-cortical connectivity may allow for the use of cues processed by POr to directly modulate semantic and

thematic content processed in PTr and POp. Presumably, such circuitry could also be instrumental for the recovery of language function following subcortical infarct, if remaining cortico-subcortical circuitry was not viable and if sufficient prior learning had occurred to promote strong connectivity at the cortical level. In the case of conflict or excessive syntactic complexity, a healthy brain's cortico-subcortical circuits would continue to allow for robust processing based on comprehensive, unfolding sentence context. This model bears some similarities to Ullman's (2004, 2006, 2016) declarative/procedural neurobiological model. Like Dominey and colleagues, Ullman describes a hypothetical cortico-striato-thalamo-cortical structural network that is instrumental for learning and verbal processing. Ullman contrasts with Dominey and colleagues, as well as Teichman et al. (2015), by specifying that this network also encompasses cortical circuitry with the anterior putamen.

The standout controversy among theoretical models of syntactic processing is that while some assign POr a key role, many others conclude that syntactic processing is likely regulated by a functional gradient across PTr and POp exclusively (e.g. Hagoort & Indefry, 2014). Some evidence for POr-driven syntactic processing can be found in the literature but is hardly conclusive. Cooke et al. (2001) manipulated grammatical structure of English sentences for an fMRI analysis of language processing and found that only POr was significantly activated for the most complex, least canonical sentences. The significance and specificity of these findings are weakened by the relatively small sample size of this study and, as the authors point out, other literature variably demonstrates recruitment of other or additional IFG regions for syntax complexity manipulations. Fiebach, Schlesewsky, Lohmann, von Cramon, and Friederici, (2005) posit an interesting hypothesis that the IFG's involvement in syntax actually represents an attentional, working memory function, as opposed to syntactic processing itself. In their German language fMRI research, increase of working memory burden compared to grammatically equivalent sentences resulted in significant BOLD signal activation in classical Broca's area, but not in POr. However, other researchers interested in localizing syntactic working memory have found evidence that POr may actually be well-suited for such a role (e.g. Dronkers, Wilkins, Van Valin, Redfern, & Jaeger, 2004). Coupled with additional research contributing to a lack of resolution regarding the

localization of verbal working memory, it is difficult to say if sub-regions of the IFG contribute differentially, or at all, to verbal working memory. Accordingly, we must ask what other cognitive processes these regions participate in that could provide unique context for attentional maintenance.

Detection and processing of prosody are not characteristically discussed as basic language functions, yet they are undeniably a part of spoken language comprehension and production. Functional MRI research over the past decade has indicated that POr may play a bilateral role in cognitive functions related to prosody (Belyk & Brown, 2013; Belyk & Brown, 2015; Buchanan et al., 2000; Fecteau, Armony, Joanette, & Belin, 2005; Frühholz & Grandjean, 2013; Merrill et al., 2012; Wildgruber et al., 2005). Furthermore, dysprosodia, dysarythia, and impaired recognition of emotional prosody are known to sometimes occur following damage to the basal ganglia (Alexander, Benson, & Stuss, 1989; Damasio, Damasio, Rizzo, Varney, & Gersch, 1982; Cancelliere & Kertesz, 1990; Mills & Spiller, 1907; Paulmann, Pell, & Kotz, 2008), suggesting that an anatomical or functional connection between POr and the basal ganglia is behaviorally reasonable. A left hemisphere prosody function could strategically enable POr to incorporate an additional layer of temporally meaningful, auditory context into semantic and syntactic judgments at both the word and sentence level. With support from the basal ganglia and the thalamus, this context could modulate semantic working memory or semantic integration in POr/PTr, while also guiding syntax-based decisions in combination with semantic and thematic information. Essentially, provided adequate cortico-subcortical connectivity exists, prosody could in part explain POr's contribution to semantic and syntactic integration without necessarily assigning POr the burden of what is traditionally held to constitute syntactic processing.

2.2 The Subcortical Brain

Cortico-subcortical circuits are far more anatomically complex than the basic cortical input and output described thus far, or that this research proposes to address with tractography. All cortical lobes of the brain have some degree of subcortical connectivity. Between the neostriatum of the basal ganglia and the thalamus, several neural pathways transmit information related to cognitive functions subcortical structures are thought to execute or support. Regarding language, these functions range from domain-

specific language faculties such as word generation to domain-general or executive processes that interact with language comprehension and production.

2.2.1 Cortico-subcortical Anatomical Circuitry

A number of cortico-subcortico-cortical loops have been described in the human anatomical literature (e.g. Alexander & Crutcher, 1990; Barbas, García-Cabezas, & Zikopoulos, 2013; Crosson, 2013; Middleton & Strick, 2000, 2001; Parent & Hazrati, 1995). Information from the cortex typically enters the basal ganglia via the neostriatum (at the putamen or the caudate nucleus), passes through the internal segment of the globus pallidus (GPi) or the substantia nigra pars reticulata (SNr), and in turn acts upon various thalamic nuclei that project back to the cortex. Slight variations to this circuitry provide additional means of thalamic communication. The external segment of the globus pallidus (GPe) receives striatal projections which rely on the subthalamic nucleus (STN) to send messages to the GPi and SNr. The cortex also communicates with the STN directly to send signals along this path, cutting the neostriatum out of the loop entirely.

Discrete basal ganglia loops comprised of this circuitry have been outlined in context of both language and motor functions (Crosson, 2013; Nambu, 2004; Nambu et al., 2000), and are thought to represent different functional contributions. The first loop to be formally described was the "direct" loop, which may increase signal for emerging behavior (e.g. word generation) at the cortical level via connectivity with the neostriatum, GPe, and thalamus. The "indirect" loop also involves afferent circuitry to the neostriatum, but is believed to suppress competing alternatives (e.g. non-intended but semantically related words) for which signal has been increased per excitation via the direct loop, with the net effect of increasing the signal-to-noise ratio of correct or intended behaviors. Finally, the "hyperdirect" loop surpasses the neostriatum to send impulses that may facilitate suppression of recently executed behaviors (e.g. a previously generated word) to assist with accurate execution of emerging behaviors (e.g. continuing to name novel words from a given category). Each of these basal ganglia loops is depicted on the following page in Figure 1.

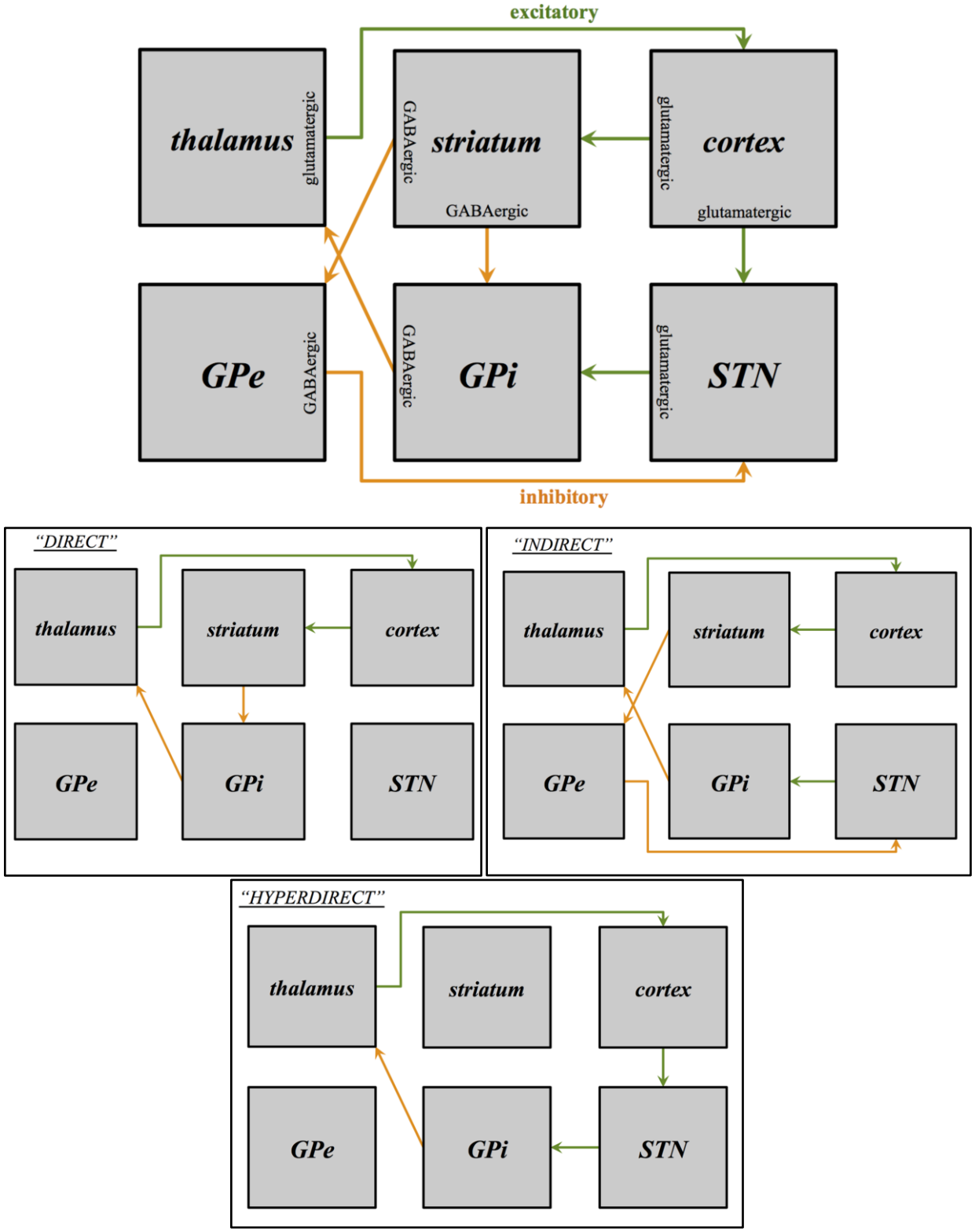

***Figure 1**. Direct, indirect, and hyperdirect basal ganglia loop overview. Green arrows represent excitatory glutamatergic projections, while orange arrows represent inhibitory GABAergic projections.*

Throughout the brain, the thalamus has direct, reciprocal circuitry with cortical regions, although not all cortico-thalamic projections are reciprocated (Sherman & Guillery, 2006). Many but not all of these projections to the cortex represent glutamatergic, excitatory subsets of the basal ganglia loops described in the previous paragraph. Discrete thalamic nuclei within the internal medullary lamina send excitatory afferents back to the striatum. Finally, much of the exterior of the thalamus is enveloped by a topographically organized layer of GABAergic, inhibitory neurons known as the nucleus reticularis. The nucleus reticularis is unfortunately not visible with current MRI technology, but is consequential for thalamic structural connectivity and function. This structure receives cortical and thalamic inputs and strategically outputs exclusively to thalamic nuclei, likely participating in a complex, interactive chain-reaction of topographically selective inhibition and activation.

This rudimentary overview of subcortical loops, although widely accepted by the scientific community, is in part based on comparative research conducted well before the development of *in vivo* technology used to examine neural circuits in humans. As noted, neuroscientists have yet to map out all of the cortico-subcortical/subcortico-cortical circuits presumed to participate in these subcortical loops. Thus, much of what is known or assumed about cortico-subcortical architecture is derived from *ex vivo* primate tracing research.

2.2.2 Primate Thalamic Circuitry

Goldman-Rakic & Porrino (1985) demonstrated that each primate frontal region receives topographically unique, clustered input from the medial dorsal thalamus with their classic, retrograde tracing study of rhesus monkeys. Similarly specific, organized projections from the ventral anterior nucleus and the medial portion of the pulvinar (mPul) are also present for all primate prefrontal regions. To quote these authors, “segregation of projections seems to be a general rule governing the organization of thalamocortical connectivity in virtually all areas of the cortex”.

Further investigation of mPul projections to the primate frontal cortex revealed both segregation and integration within the mPul for regions that are relatively homologous with the human IFG (Romanski, Giguere, Bates, & Goldman-Rakic, 1997). The cytoarchitectonic region corresponding to

POr (Walker area 12; Petrides, Tomaiuolo, Yeterian, & Pandya, 2012; Walker, 1940) receives dense, afferent projections from both medial and central/lateral regions of the mPul, while the PTr homologue and other frontal regions receive more prominent afferents from either one portion of the mPul or another. Both afferent and efferent projections from area 12 were observed and were primarily associated with cortical layer VI. Presumably, the topographical spread of primate POr homologue circuitry within the pulvinar might imply an anatomical rationale for functional similarities between POr and PTr that are not mutually exclusive from functional differences, or architecture supportive of pulvinar-driven modulation. Romanski et al. noted that all regions of the cortex which receive mPul afferents, including insular, parietal, and temporal areas, have reciprocal connections with this thalamic nucleus. The pulvinar also has direct, reciprocal connectivity with the primate visual network (Kaas & Lyon, 2007; Sherman & Guillery, 2006).

Asanuma, Andersen, and Cowan (1985) compared thalamic projections of the macaque's lateral frontal areas to thalamic projections of the inferior parietal lobule and similarly demonstrated evidence that the neuronal distributions of these regions are both segregated and comingled within mPul. Individually, mPul projections were organized in disk-like aggregates and topographically organized in relation to single gyri. Within mPul, there was a substantial region of overlap of frontal and parietal projections. However, there was a clear segregation of the distribution as well, and only a very minute portion of the projections from integrated areas appeared to actually overlap upon microscopic inspection. Taken as a whole, the primate literature suggests (1) the existence of POr-thalamic/thalamo-POr circuitry and (2) intra-thalamic topographical segregation that is not mutually exclusive from some degree of integration at the pulvinar.

2.2.3 Functions of the Thalamus

Broadly, the thalamus is proposed to participate in language processing by moderating selective engagement of relevant cortical regions, relaying information between cortices, sharpening focus on salient sensory-verbal information, and working in concert with the basal ganglia to increase speed and accuracy of word selection (Crosson, 1985, 1999, 2013). These thalamic functions are posited in

consideration of the anatomical and physiological features of neurons. The firing of efferent relay neurons can be characterized as either residing in a low-fidelity mode of frequent, rhythmic firing, or a high-fidelity mode that corresponds linearly to driving input. "Driving" axonal afferents typically originate from layer V of the neocortex and pass through the nucleus reticularis uninterrupted. In contrast, "modulating" afferents originate in cortical layer VI and send collaterals to the nucleus reticularis that then project back to the thalamus. Modulators influence thalamic relay firing via either the low-fidelity or high-fidelity mode of transfer.

The combined functioning of thalamic inputs and relays could allow for intentionally guided attention, or "selective engagement", with assistance from the pulvinar and its diffuse connectivity with the frontal, temporal, parietal, and occipital lobes. As described by Crosson (2013), selective engagement is a mechanism with which the thalamus engages cortical regions relevant to a given task or cognitive process by influencing states of neuronal transfer. High-fidelity transfer via higher-order cortical relays with driving afferents would permit the thalamus to pass information amongst cortices. Contrastingly, relays influenced by modulating input also influence the cortex of origin and facilitate change between transfer modes, permitting the sharpening of focus on salient sensory or perceptual stimuli for accurate processing. Disruption of thalamic inputs and relays associated with frontal cortices of the language network could result in a failure to integrate semantic or lexico-semantic information, leading to the semantic paraphasias characteristic of thalamic aphasia (see Section 3.1). Crosson additionally proposed that modulatory input from POr to the pulvinar may switch thalamic relays to the high-fidelity transfer mode for semantic processing, consistent with the theories discussed in Section 2.1.2 that assign a modulatory function to this region. However, Crosson's theory does not rely on striatal connectivity and is dependent on the existence of layer VI cortical afferents to the thalamus' pulvinar nucleus, a level of anatomical detail not addressed by other theories.

As described previously, some of the thalamus' language functions involve coordination with the basal ganglia. Crosson (2013) suggested that word selection in particular may be enhanced by the activity of cortico-striato-thalamic projections of cortico-subcortical loops. Each set of pathways described in

Section 2.2.1 has a unique role in the physiological excitation or inhibition of thalamic relays, collectively contributing to both enhancement and suppression of word representations for speech output. It is important to note that in Crosson's theory, language per se is not reliant on the basal ganglia, although it involves an interaction with them. Rather, an executive or supporting role in language cognition is posited for these structures.

2.2.4 Primate Basal Ganglia Circuitry

Like the thalamus, the primate basal ganglia appear to be well linked to Walker's area 12, the cytoarchitectonic region most correspondent to POr in humans (Petrides et al., 2012; Walker, 1940). In the late 20th century, evidence that area 12 projects to the ventromedial portion of the caudate nucleus began to surface (Alexander, DeLong, & Strick, 1986; Arikuni & Kubota, 1986). These two groups' evidence differed in that Arikuni and Kubota also found projections in the central portion of the caudate nucleus and terminals were exclusive to the head, while Alexander and colleagues specified fibers along the length of this structure, from head to tail. Of note, Alexander et al.'s discussion grouped areas 10 and 12 together, possibly contributing to discrepancies. At around the same time, Selemon and Goldman-Rakic (1985) demonstrated that primate homologues of BAs 4, 6, 9, 10, 11, and 12 of the frontal lobe each project to both the caudate nucleus and the putamen. Middleton and Strick (2000, 2001) later elaborated on the area 12/POr fronto-striatal circuit after more evidence had accumulated, asserting that projections from the ventromedial head of the caudate nucleus output to the substantia nigra and ultimately pass through the medial dorsal and ventral anterior nuclei of the thalamus.

Haber, Kunishio, Mizobuchi, & Lynd-Balta (1995) also scrutinized macaque basal ganglia connectivity, by examining retrograde tracing from injections into the caudate nucleus, putamen, and nucleus accumbens as well as anterograde tracing from the frontal cortex. Very few terminations were found in the dorsolateral putamen. Lateral ventral striatum injections resulted in few visible terminations, and those which were observed resided primarily in layer V. Injections into the medial central striatum, a portion of the caudate nucleus, had terminals scattered throughout layers V and VI. Finally, a region of the central, ventral striatum that spanned the ventral caudate nucleus and ventral medial putamen received

projections from “most of area 12”, primarily from layers V and VI but also sparsely from layer III. Broadly, Haber and colleagues’ reported that projections from the frontal brain had terminals extending throughout the head and body of the caudate nucleus, which they described as consistent with Selemon and Goldman-Rakic’s (1985) previous findings. The nucleus accumbens, which is also subsumed by the primate ventral striatum, was not noted to have any area 12 projections, however afferents from area 13 were dense. Each of the regions cited prior as having area 12 projections contained area 13 projections as well. Walker’s areas 12 and 13 collectively constitute the homologue of human BA 47, however even in humans there is a cytoarchitectonic distinction between these regions (Petrides et al., 2012). Area 12 is more consistent with the POr gyral region due to its lateral positioning and sulcal boundary at the lateral orbital sulcus. In contrast, area 13 is set more medially. Although some overlap is possible and expected when comparing gyral regions to cytoarchitectonic regions, POr is better represented by Walker’s area 12.

Overall, the primate literature suggests that POr has structural connectivity with both the caudate nucleus and the putamen. Putaminal terminals appear to primarily be situated medially, and caudatal projections may be more densely distributed. It could be that the etiology of this imbalance between projections to the caudate nucleus versus the putamen relates, in part, to findings that the more anterior region of the putamen bears more similarities to the caudate nucleus, structurally and functionally, than the more posterior regions (Selemon & Goldman-Rakic, 1985). In primates, the majority of the putamen is diffusely and densely connected to the motor and sensory cortices, but not to frontal regions directly associated with higher-order cognitive functions and language (Whitworth, LeDoux, & Gould, 1991).

2.2.5 Functions of the Basal Ganglia

The basal ganglia’s language functions have been subject to debate, with some considering the notion that they only have a secondary impact on language (e.g. Crosson, 2013; Damasio et al., 1982), in contrast with a more foundational role in the language network. Discussion of the basal ganglia’s relevance to language processing has persisted for decades (e.g. Braaten, Moore, Cooley, & Stringer, 2011; Brunner, Kornhuber, Seemüller, Suger, & Wallesch, 1982; Copland, Hons, Chenery, & Murdoch,

2000; Damasio & Geschwind, 1984; Fabbro, Clarici, & Bava, 1996; Kotz et al., 2003; Wallesch, 1985; Wallesch et al., 1983), but without one side of the debate ever entirely prevailing over the other.

This controversy appears to be mostly a debate of definition; defining the basal ganglia as language structures implies to many that they are poised to execute domain-specific language functions. To date, evidence does not indicate that this is the case (see Section 3.2). Rather, the basal ganglia appear to be involved in higher-order, domain-general cognitive functions or executive processes that strongly influence language behaviors and processes. But given a systems approach to cognition and behavior, domain-general processes that direct language are no less relevant or essential to the study of language than domain-specific processes.

Further, striatal executive processes likely mediate language faculties as a function of development, highlighting the basal ganglia as an important set of structures in the clinical consideration of language. Research examining basal ganglia volumetry in children with attention-deficit hyperactivity disorder (ADHD), a clinical disorder characterized by executive functioning weaknesses, reveals a significant pattern of decreased volume of the head and body of the caudate nucleus and the anterior putamen, although mostly or exclusively in male cohorts (Hynd et al., 1993; Qiu et al., 2009). Developmental language disorders' (LD) high incidence of co-morbidity with ADHD is well established and suggests a link between executive processes and the development of certain verbal skills (American Psychiatric Association, 2013; Martinussen, 2015), although ADHD can and does occur independently from LD. Further support for the basal ganglia's role in mediating language development is found in childhood lesion studies that paint a profile of language deficits much more extensive and domain-specific than typically found in the adult lesion literature (see Section 3.2).

3 LANGUAGE AND SUBCORTICAL LESIONS

3.1 Thalamic Lesions

Thalamic lesions are peculiar in that they almost invariably lead to semantic deficits during word generation or naming (Crosson, 2013). Raymer, Moberg, Crosson, Nadeau, and Gonzalez Rothi (1997)

hypothesized that the semantic deficits of thalamic aphasia are a result of failure to integrate semantic and lexical information. Less consistently, deficits in other domain-specific language functions such as reading, comprehension, and repetition have been documented. Syntactic or grammatical deficits are uncommon, differentiating thalamic aphasias from non-fluent aphasias due to cortical damage. Both infarcts and hemorrhages typically result in transient symptoms, although infarcts tend to result in more variable symptomology. The nature of symptoms is also partially dependent upon which thalamic nuclei are compromised, although damage to different nuclei can lead to similar deficits. Infarcts to the ventral anterior and ventrolateral nucleus, regions typically supplied by the tuberothalamic artery, tend to be consistent in producing paraphasias (Wallesch, 1997). Nishio et al. (2014) posited that deficits subsequent to anterior lesions result from widespread disconnection of various tracts that intersect at the ventral anterior nucleus. Albeit less consistently, pulvinar lesions also appear to result in semantic deficits (e.g. Crosson et al., 1986; Crosson, Moberg, Boone, Gonzalez Rothi, & Raymer, 1997; Raymer et al., 1997). This variability may be partially related to lesion positioning within sub-regions of the pulvinar, which notably have been shown to have distinct structural connectivity patterns in primates (Romanski et al., 1997). Transient language deficits related to object naming and recollection have been produced with electrode stimulation to both the pulvinar and the ventrolateral nucleus, further substantiating these nuclei's importance for language behaviors (Ojeman, 1975). The anterior nucleus, mediodorsal nucleus, ventroposterior nucleus, ventroposteriolateral nucleus, intralaminar nuclei, and other thalamic nuclei have also been variably implicated for language functions (Barbas et al., 2013; Crosson, 2013; Nishio et al., 2014; Wallesch, 1997).

3.2 Basal Ganglia Lesions

Much of the hesitance to label the basal ganglia as key structures in the language network owes to adult stroke research that indicates otherwise. Nadeau and Crosson (1997) argued against any major, direct language role or mechanism of disconnection or diaschisis leading to non-thalamic, subcortical aphasia syndromes. Rather, they asserted that cortical hypoperfusion subsequent to vascular events were responsible for aphasia after basal ganglia infarct. Hillis et al. (2002) substantiated these findings by

demonstrating that every subject in their study with both an isolated subcortical lesion and accompanying aphasia also presented with prominent cortical hypoperfusion in the middle cerebral artery (MCA) territory, with 9 of these subjects having an isolated, left caudate nucleus infarct. Language deficits were not observed for subjects with similar lesions unaccompanied by MCA territory cortical hypoperfusion. Additionally, the language performance of every subject with subsequently restored perfusion was recovered or improved. At first glance these results are compelling, however a deeper look reveals several limitations to the generalizability of their results. Every subject was initially recruited and tested during the acute phase of stroke (≤ 24 hours), and those studied after perfusion was restored were retested within just 3 days. However, stroke is dynamic, evolving physiologically and behaviorally over a much more extended period. Additionally, none of the subjects with thalamic infarcts had detectable language deficits, although it has been established that the thalamus has a prominent role in language processing. Hillis et al. note that this null finding may be a result of an impoverished test battery unable to detect deficits specific to thalamic aphasia due to its sole focus on lexical aspects of verbal cognition. This methodological flaw is concerning given Raymer et al.'s (1997) conclusion that both semantic and lexical processing are independently spared in the face of thalamic infarct, while instead modal integration of these faculties is interrupted. It is also possible that Hillis and colleagues' subjects had damage to portions of the thalamus that are not connected to cortical areas of the language network. Reasonably, these confounds might apply to subjects with basal ganglia infarcts as well.

Copland and colleagues (2000) actually demonstrated two years prior that traditional aphasia batteries are not sufficient for revealing language deficits of patients with basal ganglia lesions. The Western Aphasia Battery (WAB) was not sensitive to language deficits in their study's patients, however other tasks such as synonym and antonym generation, extracting meanings from ambiguous sentences, and others showed significant differences compared to controls. Braaten et al. (2011) presented the case of a 70 year-old man examined 3 months following infarct to his left caudate nucleus, putamen, and globus pallidus. This man spoke fluently, performed within normal limits on the WAB, and had intact comprehension, grammar, syntax, and articulation. However, on tasks of verbal fluency, confrontation

naming, and word list learning, his performance was borderline to extremely low (2-3 SD below the mean), indicating verbal impairment. Additionally, his performance indicated marked perseveration on executive functioning tasks such as card sorting. It is worth noting that some of these features, in particular word-selection deficits, are consistent with Crosson's (2013) theory that basal ganglia loops contribute to efficient and accurate word generation. Other observations more generally accompanying adult basal ganglia infarcts include articulation errors, dysprosodia, word-finding problems, and grammatical speech that is casually fluent but impacted in the face of complex syntax (reviewed by Ardila, 2010). Foreign Accent Syndrome, a rare neurological condition characterized by acquired changes in speech articulation patterns, is thought to be associated with putaminal lesions (reviewed by Abutalebi et al., 2013). Altogether, such findings strongly suggest that although basal ganglia damage in adulthood may not lead to traditional aphasia syndromes, notable language-related deficits present and should be further addressed academically and clinically.

The prior cited literature's conclusions are exclusively based on adult stroke patients, however stroke occurs in childhood as well. Gout et al. (2005) demonstrated that children with early childhood basal ganglia infarcts may present with features common to both frontal cortical and subcortical aphasias in adults. Their subjects' acute symptoms included non-fluent aphasia, mutism, hypospontaneity, neologisms, phonemic and semantic paraphasias, and word finding difficulties. Other observed deficits involved reading, writing, repetition, and spelling. Later onset (school age versus younger) resulted in more favorable outcomes. These authors also emphasized the dynamic nature of subcortical aphasia in their research subjects; although some symptoms variably improved, other deficits presented years later in development as verbal expectations changed. As such, disruption of the domain-general functions of the basal ganglia may have directly impacted the acquisition/development of domain-specific language skills.

3.3 Relevance to Present Research

Discussion of stroke research is of two-fold necessity when considering the anatomical circuitry of behavioral networks in healthy subjects. Most intuitively, a great deal of what is known about functional neuroanatomy was learned via lesion studies. The consequences of localized damage speak to

a region's behavioral relevance, indicating why scientists should concern themselves with mapping out that region's circuitry with tractography. In other words, stroke research may indicate which projections are likely to constrain behavior in a given way. Studying stroke-induced subcortical aphasias has clued us into which subcortical circuits might support the language network for healthy, typical verbal functioning, and more specifically what sorts of verbal processes subcortical circuits might support. Thalamic aphasia research seems to indicate that cortico-thalamic/thalamo-cortical structural connectivity with the IFG primarily supports verbal integration. Basal ganglia circuitry with the IFG is likely relevant for maintenance of domain-general or executive processes affecting speech execution and planning, along with the development and utility of specific language skills.

Conversely, establishing baseline expectations is critical for understanding clinical deviations from healthy circuitry. By nature, stroke leads to localized loss of brain matter. In depth knowledge of exactly which networks once passed through damaged regions or nuclei can only be ascertained from healthy brains with intact structural connectivity. Of course, individual differences in neuroanatomy are commonplace and expected. Detailed topographical expectations are therefore necessary in order to make predictive assumptions about which circuits will be interrupted subsequent to subcortical events. Where circuitry is segregated, it may be possible for adjacent networks to assume behavioral functions for the promotion of language recovery. In contrast, where circuitry is integrated or relatively overlapping, it is more likely that a vascular event would compromise white matter projections of multiple regions. In this context, the potential substrates for neuroplastic mechanisms supporting language recovery might change or become more limited.

4 SPECIFIC AIMS

4.1 Cortico-striatal Circuitry

The first specific aim of this thesis addressed the hypothesis that there is direct, cortico-striatal, structural connectivity between the IFG and the neostriatum of the left hemisphere. Afferent projections

from POr, PTr, and POp to the putamen were expected to approach the anterior-superior portion of the putamen in the anterior portion of the internal capsule. Caudate nucleus projections were expected to enter the caudate at either the head or the body, also in the anterior portion of the internal capsule.

Ford, Triplett, et al. (2013) previously demonstrated the presence of robust structural connectivity between Broca's area (PTr/POp) and the anterior portion of the putamen, but were unable to confidently replicate low-angular tractography findings of possible caudatal circuitry (Lehéricy et al., 2004) using contemporary, high-angular methods. This thesis applied an innovative, intra-structural framework to direct networking of high-angular deterministic tractography (Appendix B), theorizing that network tracing optimization might enable more robust detection of caudatal networks, should they exist.

4.2 Cortico-thalamic/thalamo-cortical Circuitry

The second specific aim addressed the hypothesis that there is direct, cortico-thalamic/thalamo-cortical, structural connectivity between the IFG and the thalamus. Subcortical circuitry of POr, PTr, and POp was expected to meet the thalamus at the ventral anterior nucleus, within the genu of the internal capsule. Intra-thalamically, these networks were expected to extend throughout the internal medullary lamina and into the pulvinar nucleus.

Prior investigations have demonstrated the feasibility of tracing streamlines between Broca's area and the thalamus (Ford, Triplett, et al., 2013) as well as segmentations of the thalamus' ventral anterior and pulvinar nuclei (Bohsali et al., 2015) with direct, structural networking. This thesis' investigation of PTr and POp subcortical circuitry was conducted to replicate these findings in an intra-structural networking framework, while generating data for the third specific aim.

4.3 Intra-thalamic Network Integration/Segregation

The final specific aim was to describe and quantify the intra-thalamic topography of cortico-thalamic/thalamo-cortical networks. It was predicted that within-subject groups of cortical regions would demonstrate some overlap along network borders, but that circuits would predominantly occupy distinct,

segregated spaces within the thalamus. Please note for the purpose of clarity that network overlap is also discussed as "integration".

Each of the described aims was systematically addressed within a high-angular, deterministic DWI framework using a mixture of Wisharts (MOW) fiber reconstruction method for global estimation of white matter circuitry.

5 MIXTURE OF WISHARTS FIBER RECONSTRUCTION

Jian and colleagues (Jian & Vermuri, 2007a, 2007b; Jian, Vermuri, Özarslan, Carney, & Mareci, 2007) proposed a robust statistical method for modeling white matter pathways by representing local diffusion as a MOW probability distribution. This model is used in conjunction with a non-negative least squares (NNLS) spherical deconvolution algorithm to address the issue of multiple fiber orientations in complex microstructures crossing or diverging within voxels. Experimental results showed that this framework outperforms other high-angular, deterministic techniques for multi-fiber reconstruction and is more resistant to noise in the diffusion-weighted signal.

The accuracy and utility of this framework for estimating cortico-thalamic/thalamo-cortical and putaminal fibers within the language network has been demonstrated in the past by Bohsali and colleagues (Bohsali et al., 2015; Ford, Triplett, et al., 2013) for the PTr and POp cortical regions, as noted in previous sections. These scientists' work is particularly demonstrative of the sensitivity of this deterministic method because the capsular fibers connecting Broca's area to the thalamus and putamen pass the more robust pathways of the arcuate fasciculus and superior longitudinal fasciculus after emerging past the circular sulcus of the insula, in addition to crossing paths with fibers linking Broca's area to the medial frontal cortex (Ford, McGregor, Case, Crosson, & White, 2010). Bohsali et al. also demonstrated that this method is capable of reproducing visual pathways known to connect the optic chiasm, the lateral geniculate nucleus (LGN) of the thalamus, and the occipital cortex. Additionally, members of these research groups successfully derived maps of white matter pathways in the human brainstem, a region notable for its dense, complex neural architecture (Ford, Colon-Perez, et al., 2013).

To our knowledge, no prior diffusion research has investigated the subcortical circuitry of POr within this framework. A literature search for subcortical tractography of POr using other fiber reconstruction and modeling methods yielded similarly absent results, notwithstanding Lehéricy et al. (2004)'s preliminary finding of possible caudate nucleus connectivity.

6 METHODS

6.1 Participants

This research utilized MRI data acquired previously by collaborators and mentors in the author's research lab at the Atlanta VA Medical Center. The sample included 11 healthy, right-handed, young-adult volunteers with a mean age of 24.7 years (range = 21-31; female, $n = 5$; male, $n = 6$).

Data collected from nine additional subjects were excluded from analyses. Five of these subjects' acquisitions were unusable due to excessive head motion. One subject was improperly positioned in the MRI scanner. The other three subjects either presented with underlying medical conditions with the potential to adversely affect neural architecture or were atypical anatomical variants. Each of the former was evaluated by a neuroradiologist prior to exclusion. It is worth noting that one subject who was not excluded (#8) reported prior drug abuse and had an unexpected adverse reaction to transcranial magnetic stimulation (TMS) of the cerebral cortex. TMS was applied subsequent to scanning and for research carried out independently from this analysis.

6.2 Data Acquisition and Processing

Diffusion-weighted images were acquired axially on a 3T Siemens Trio scanner with a 32-channel head coil, using spin-echo echo planar imaging (EPI) in the anterior-to-posterior phase encoding direction and GRAPPA parallel imaging (acceleration factor of 2), for 64 slices, FOV = 256 mm x 256mm, TR = 8900ms, TE = 99ms, flip angle = 90°, and voxel size = $2mm^3$, for a 10min 7sec acquisition. The diffusion weighting gradients were distributed using a 64-direction acquisition scheme with b = 1000 s/mm^2. One un-weighted volume (b = 0 s/mm^2) was acquired prior to applying gradients. Structural, T1-

weighted MPRAGE scans were collected with 176 sagittal slices, FOV = 256mm x 256mm, TR = 2300.00ms, TE = 2.89ms, and voxel size = $1mm^3$. Additionally, a functional MRI field map collected during a resting state (rfMRI) was acquired with 55 interleaved axial slices in the right-to-left phase encoding direction, FOV = 220mm x 220mm, TR = 582.00ms, TE = 4.92/7.38ms, flip angle = 60°, and voxel size = $3mm^3$.

Diffusion-weighted volumes were pre-processed to linearly correct for motion and shearing or stretching artifacts across gradients using the FMRIB Software Library (FSL) (Smith et al., 2004). Skull-stripping of the T1-weighted images and diffusion-weighted scans was performed using the FreeSurfer neuroimaging software suite and the FSL-VBM brain extraction module (see Appendix A). The DTIFIT module of FSL's diffusion toolbox (FDT) was used to generate an ordinary least squares model of the diffusion tensor at each voxel, for visualization and quality control.

White matter fiber tract orientation was estimated based on a MOW signal attenuation model (Jian & Vemuri, 2007a, 2007b; Jian et al., 2007). This reconstruction method estimates tracts of all neural pathways in the brain according to manually specified parameter restrictions. The highest probability maxima of water molecule displacement, shown to correspond with fiber orientation, were saved along five directions given a minimum probability threshold of 50%, for tracking 3D streamline vectors of over $1nm^3$ point resolution. Streamline tractography was performed with software developed by Dr. Thomas Mareci's research group at the University of Florida (http://marecilab.mbi.ufl.edu). In consideration of the heterogeneous composition of subcortical brain structures and relative lack of FA differentiation between some subcortical and ventricular regions, no FA thresholding was applied to this thesis' data. Each $2mm^3$ voxel was seeded with a sub-voxel grid consisting of 64 evenly-spaced seed points. A sub-voxel grid of 64 seed points per $2mm^3$ of space was determined to be sufficient and optimal based on the inherent limitations of existing technology, as well as Bohsali and colleagues' (2015) previous success with this parameter for mapping cortico-subcortical fibers from 3T MRI scans acquired at $2mm^3$ resolution. From each seed within a given sub-voxel grid, streamlines were launched bi-directionally whilst stepping 0.25mm in the direction of local maxima of the tensor distribution. When

angular deviation of linear vectors between two consecutive step intervals exceeded 50°, tracking of that streamline was ceased. Angular deviation and step interval parameters were guided by previous investigations and chosen after *ad-hoc* data exploration.

Processing of network tractography was performed by filtering pathways to retain only the subsets of streamlines with points along an edge between region of interest (ROI) nodes (Colon-Perez, Spindler, et al., 2015). Doing so refined networks to relevant streamlines, allowing for exclusive networking of direct structural connectivity. To increase the probability of detecting a robust representation of the underlying anatomy and visualize complex pathways within the outer boundaries of ROIs, the aggregate surface area of each ROI was increased for processing by "dicing" ROIs into smaller units with in-house software developed by the author and her research team (see Appendix B).

6.2.1 Within-subject Co-registration

The T1-weighted, anatomical images were registered two different ways in preparation for ROI application. First, the T1-weighted images were aligned along the anterior to posterior commissure line (ACPC) using FLIRT rigid-body registration (6 *df*) to the Montreal Neurological Institute standard brain (MNI152), for unbiased determination of medial boundaries (Jenkinson, Bennister, Brady, & Smith, 2002; Jenkinson & Smith, 2001). Second, the native-space, T1-weighted images were co-registered to diffusion space using a three-step, semi-automated, boundary-based co-registration procedure.

Prior to co-registration, un-weighted diffusion volumes were upsampled without interpolation from $2mm^3$ to $1mm^3$ resolution using Analysis of Functional Neuroimages tools (AFNI; http://afni.nimh.nih.gov). For the initial step of the co-registration procedure, the upsampled, diffusion-weighted images were intermediately co-registered to the T1-weighted images using an rfMRI fieldmap to correct for EPI-induced distortion, as field inhomogeneities that affect functional imaging are similar to those that affect diffusion imaging. Next, the intermediately co-registered images were manually scaled, translated, and rotated as necessary to achieve cortical and ventricular alignment, prior to automated, boundary-based registration with Freesurfer. The resulting affine matrices and warp fields were used to register native, T1-weighted images, and all ROI masks segmented from them, into $1mm^3$ diffusion space.

The co-registered, T1-weighted images were downsampled from $1mm^3$ to $2mm^3$ resolution using AFNI re-sampling tools. ROI masks were converted from $1mm^3$ to $2mm^3$ resolution using FLIRT rigid body registration (6 *df*) and spline interpolation. Interpolated masks were thresholded to exclude voxels with less than 50% agreement after interpolation, and then binarized for further processing.

6.2.2 Between-subject Normalization

Individual subject data was also registered into a common space by normalizing each subject's T1-weighted image to the MNI152 standard brain. To achieve optimal subcortical alignment, an automated, three-step registration process was used. An affine linear registration (12 *df*) into MNI152 standard space was used for the initial translation. The resulting affine matrix was applied to a mask including both the brain itself and subcortical ROIs (see Section 6.2.4) for the next step. A second, affine linear registration (12 *df*) was weighted using the translated mask of the brain with subcortical ROIs, to influence and improve subcortical alignment. Finally, the twice linearly-aligned brain and brain mask were normalized to the MNI152 standard brain using FSL's FNIRT for non-linear registration (Andersson, Jenkinson, & Smith, 2007). FSL utilities were used to skull-strip the normalized brains with their corresponding brain masks, and then generate a study-specific template brain by averaging all subjects' brains into a single, normalized image. Finally, the intermediary files created by this process and within-subject registrations were used to normalize network tractography data, subsequent to processing, for thalamic circuit visualization.

6.2.3 Cortical Regions of Interest

Masks of POr, PTr, and POp for each subject were drawn manually on T1-weighted images, in native space, with ITK-SNAP software (Yushkevich et al., 2006; http://itksnap.org) by the author (SRR) and two collaborating scientists (JHD & SMT) who had expertise pertaining to this study's ROIs (see Figure 2). Each ROI was drawn by two raters, resulting in two sets of ROIs per region. Rater SRR drew masks of all ROIs for each subject, SMT drew all POr masks, and JHD drew both PTr and POp masks. All white matter adjacent to grey matter cortical regions, drawn through to the medial boundaries depicted

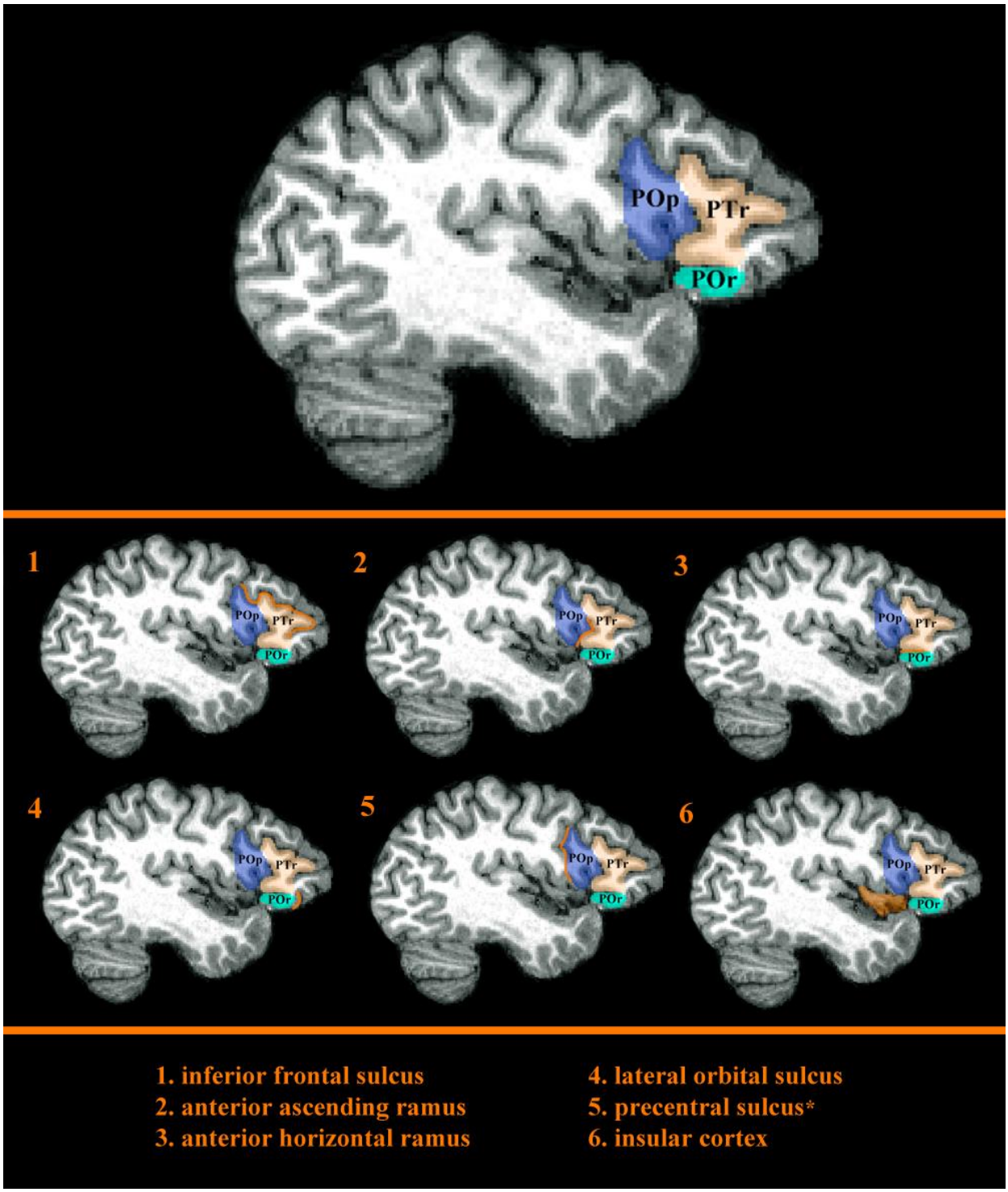

** The precentral sulcus has been extended through white matter, for visual clarity.*

Figure 2. ***Sagittal representation of pars orbitalis (POr), pars triangularis (PTr), pars opercularis (POp), and respective sulcal and structural borders, on a native-space, T1-weighted image.***

by Figure 3, was included to increase the likelihood of obtaining robust tractography results. Prior to drawing, all three scientists participated in a training and consensus session to determine standard operating procedures (SOP) for all subjects. This session involved identifying sulcal boundaries for all three ROIs and right hemisphere homologues on four archival images, each a healthy young adult, and coming to a consensus about ambiguous boundary decisions.

Inter-rater discrepancies between renderings of this study's ROIs were grossly evaluated with consideration of sulcal landmarks, and agreement was quantified with Dice similarity coefficients (DSC). The DSC formula provides a comparison of spatial overlap and is commonly used to determine inter-rater agreement and reliability (e.g. Colon-Perez, Triplett, Bohsali, Corti, & Nyugen, 2015). ROIs with a DSC of 0.70 or greater, after co-registration into $2mm^3$ diffusion space (as described above), were conflated. When spatial overlap was judged to be inadequate based on DSC values and/or observable discrepancies, the raters and an additional party with anatomical expertise (BAC) met and came to a consensus about individual subject SOP. As relevant, raters revised their ROI masks based on the established SOP prior to conflation, or the union of the two original drawings was accepted. After co-registration and downsampling into $2mm^3$ diffusion space, manual edits were performed by SRR on conflated images to ensure a one-voxel boundary between ROIs was maintained and thus to prevent overlap in streamline estimations. Additionally, any voxels positioned within the skull or meninges were eliminated.

Bohsali et al. (2015) and Ford, Triplett, et al. (2013) defined the anterior, posterior, medial, and lateral boundaries of Broca's area, respectively, as a coronal slice through the anterior margin of the anterior horizontal ramus, the inferior precentral sulcus, the first sagittal slice passing through the insular cortex, and the lateral-most slice of the frontal cortex. The anterior boundary of POp, and subsequently the posterior boundary of PTr, was defined as the anterior ascending ramus of the Sylvian fissure. In order to replicate Ford et al.'s findings, similar landmarks were used for this thesis (see Figure 3). Our boundaries differed medially in that the sagittal slice midway between the most medial and most lateral slices passing through the circular sulcus adjacent to the insula was the cortical cutoff. When a single slice did not lie midway in this range, the more lateral slice was used as the boundary. The purpose of

this deviation was to include a greater number of voxels to network from and thus increase the likelihood of obtaining robust streamlines. All medial boundaries were drawn on ACPC aligned images to prevent unsystematic differences between subjects due to head positioning during acquisition.

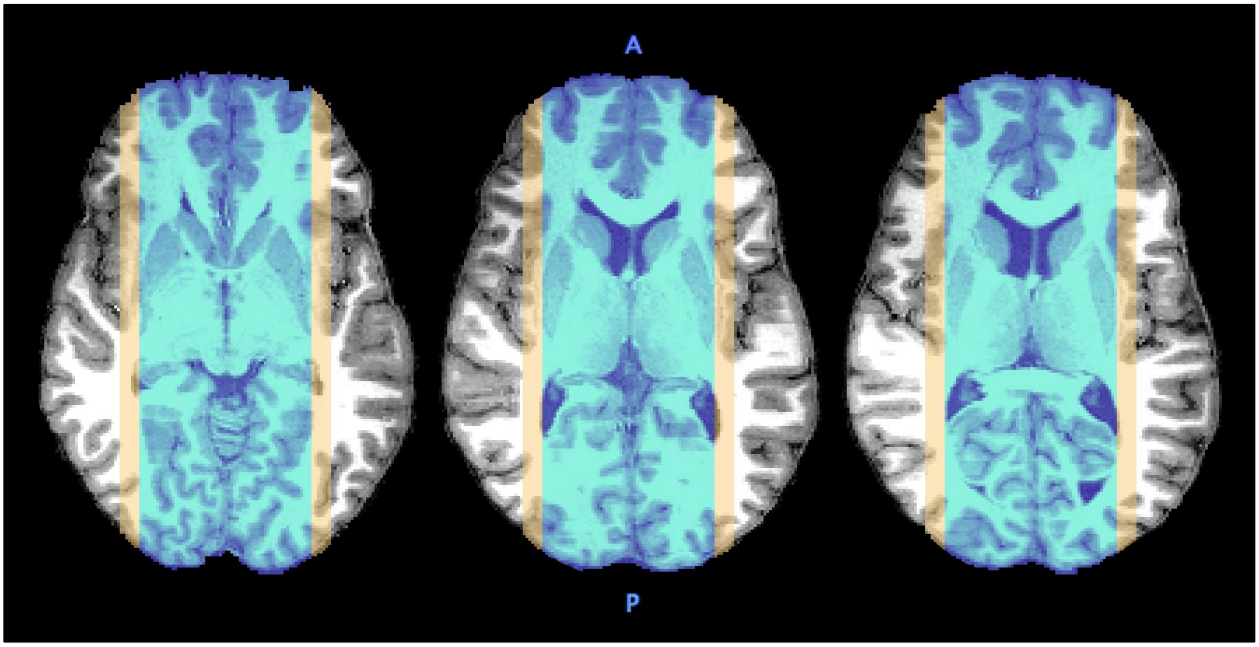

***Figure 3**. Axial slices from an ACPC aligned, T1-weighted brain scan. The medial cutoff for segmentations of pars orbitalis (POr) is represented by the outer edge of the blue shading, while the medial cutoff for pars triangularis (PTr) and pars opercularis (POp) is represented by the outer edge of the orange shading.*

Pars orbitalis (POr) is bordered anteriorly/superiorly by the inferior frontal sulcus, posteriorly/superiorly by the anterior horizontal ramus of the Sylvian fissure, and anteriorly/inferiorly by the lateral orbital sulcus (Amunts, & Roberts, 2009; Desikan et al., 2006; Keller, Crow, Foundas). The anterior/medial boundaries of POr have also been described as extending past the lateral orbital sulcus into the frontal operculum and extending into a more medial territory, resulting in distinguishable "lateral and opercular zones" (Belyk, Brown, Lim, & Kotz, 2017) that collectively better reflect the region homologous with BA 47. However, these lateral and opercular zones are also established as corresponding to cytoarchitectonically and functionally different regions in both humans and primates (Petrides & Pandya, 2012), and have been shown to have divergent striatal connectivity patterns in

macaques (Haber et al., 1995). Thus, the more conservative definition of POr analogous with Belyk and colleagues "lateral zone" was considered as an independent region for this thesis. The circular sulcus of the insula also reliably borders the "lateral zone" of POr, medially and posteriorly. To avoid potentially excluding viable voxels containing streamlines, the circular sulcus of the insula was used as a gross, anatomical landmark for the medial border of POr, instead of the medial boundary described for PTr and POp. Specifically, this border was defined as the medial-most sagittal slice containing the circular sulcus on ACPC aligned T1-weighted images (Figure 3).

6.2.4 Subcortical Regions of Interest

Segmentation of subcortical ROIs was performed using FSL's FIRST subcortical segmentation tool (Patenaude, Smith, Kennedy, & Jenkinson, 2011) to create masks of the caudate nucleus, the putamen, and the thalamus. All FIRST segmentations were used for between-subject registration weighting (see Section 6.2.2). Masks of the entire thalamus were used for data processing, allowing for intra-thalamic streamlines to be traced and analyzed without making *a priori* assumptions regarding locations of fiber termination or origin.

Prior to co-registration into diffusion space, caudate nucleus segmentations were manually edited to eliminate portions of the caudolenticular grey bridges bordering this nucleus. Given the current limitations of MRI technology, including these regions would likely result in estimating capsular fibers projecting to or from the thalamus, obscuring streamlines representing afferent fibers from the IFG to the caudate nucleus. Afferent frontal projections from the pre-supplementary motor area (pSMA) to the grey bridges have been documented in the macaque literature (Inase, Tokuno, Nambu, Akazawa, & Takado, 1999), however Inase and colleagues also demonstrated the existence of pSMA projections to the caudate nucleus, and projections of the adjacent supplementary motor region (SMA) are not as prominent within the grey bridges as they are in the primary basal ganglia structures themselves. Thus, prior findings of frontal structural connectivity with the grey bridges were not considered to be sufficient rationale for including these structures along with the risk of capsular volume averaging.

Spline interpolation to downsample from $1mm^3$ to $2mm^3$ space, during within-subject co-registration from T1-space, resulted in masks including voxels of the massa intermedia, a structure that lies in the mid-sagittal region of the brain and connects the thalamic hemispheres of most individuals (Sen, Ulubay, Ozeksi, Sargon, & Tascioglu, 2005). Although no known research to date has suggested the presence of fibers passing through this structure, likely volume averaging in this narrow region could result in the inclusion of spurious fibers from the contralateral hemisphere. To account for this, voxels included in spline-interpolated, thresholded masks of both the left and right hemispheres were eliminated prior to analyses.

6.2.5 Exclusionary Regions

When necessary, exclusion planes and exclusion masks were applied to eliminate streamlines that did not pertain to the specific aims of this research. Exclusions included neighboring regions with known or feasible structural connectivity with the ROI and/or specific exclusion planes. The medial, posterior, inferior, and superior exclusion planes were defined as follows: the mid-sagittal slice, the coronal slice 2 voxels posterior to the subcortical mask, the axial slice 2 voxels below the subcortical mask, and the axial slice 2 voxels above the corpus callosum. Neighboring gyral regions used for exclusion included other cortical ROIs and combinations of the following regions, drawn directly on $2mm^3$ diffusion-weighted images: the middle frontal gyrus, the lateral orbital gyrus, the superior temporal gyrus, the insula, and the motor cortex posterior to POp. Thalamus masks were used as exclusions for striatal networks, as although there may be genuine striatal fibers along this trajectory (Sadikot & Rymar, 2009) they do not pertain to the aims of this thesis. Striatal masks eroded one layer with AFNI tools were used to eliminate streamlines passing through adjacent striatal regions (e.g. eroded caudate nucleus masks were applied as exclusionary for putamen networks). The regions lateral to the putamen were excluded as streamline termination regions, to prevent inclusion of irrelevant streamlines while retaining streamlines entering the putamen via unanticipated routes. Finally, if it was determined with visual inspection that all streamlines remaining subsequent to exclusions failed to reach an ROI (e.g. if every streamline terminated in a

capsular voxel adjacent to a subcortical structure), that data was not recorded as a representation of structural connectivity.

6.2.6 Density Maps

Density maps that represent the number of streamlines passing through each brain voxel were created for each network, after application of exclusionary criteria. These maps are useful for analysis because they are compatible with FSL and other software that read the Nifti file format. In addition to full brain density masks, masks that only included voxels within the thalamic ROIs were generated, binarized, and combined for each subject. Prior to binarization, all density masks were thresholded with FSL utilities to exclude voxels with only a single streamline passing through them for a given network. This thresholding decreases the probability that voxels with an insignificant streamline presence do not inflate quantitative values derived from density masks. Figure 4 illustrates a 2D rendering of this scenario to demonstrate why it is intuitive to eliminate these streamlines from our model. As you can see, this hypothetical set of pixels contains streamlines from two separate networks that do not appear to overlap. Post-thresholding, the pixel on the bottom right would not be designated as a region of overlap for these two networks, and thus would better represent the underlying anatomy.

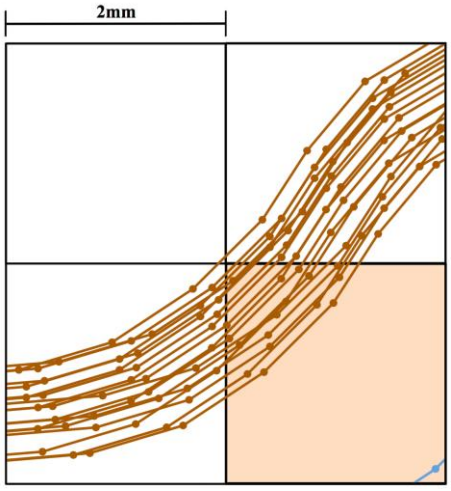

Figure 4. ***2D pixel representation of 2mm^3 voxels. Streamlines from two separate, hypothetical networks are depicted. One of these networks (blue) has only a single, trivial streamline that passes through the bottom right pixel. The entire bottom right pixel would be designated as a region of overlap (shaded) in the absence of thresholding, although the two networks occupy distinct spaces.***

6.3 Data Analysis

6.3.1 Cortico-striatal Circuitry

Subcortical streamline projections from the IFG to the neostriatum were predicted to terminate in both the anterior-superior portion of the putamen and the head or body of the caudate nucleus. Anatomically valid capsular projections could be expected to bear resemblance across subjects. Qualitative information pertaining to striatal circuitry was recorded for each network generated from POr, PTr, and POp. In consideration of Ford, Triplett, and colleagues' (2013) report of caudatal streamlines which approached the caudate nucleus but appeared to best represent capsular fibers en route to the thalamus, attention was given to whether or not streamlines in caudatal networks appeared to genuinely enter this structure or rather simply brush past it, as in the latter case those streamlines might represent neighboring cortico-thalamic/thalamo-cortical fibers or be a product of volume averaging. Specifically, for a network to be considered reflective of genuine cortico-caudatal fibers, there must have been streamlines that reached beyond the lateral-most 2mm^3 voxels of the caudate nucleus ROI mask (Figure 5).

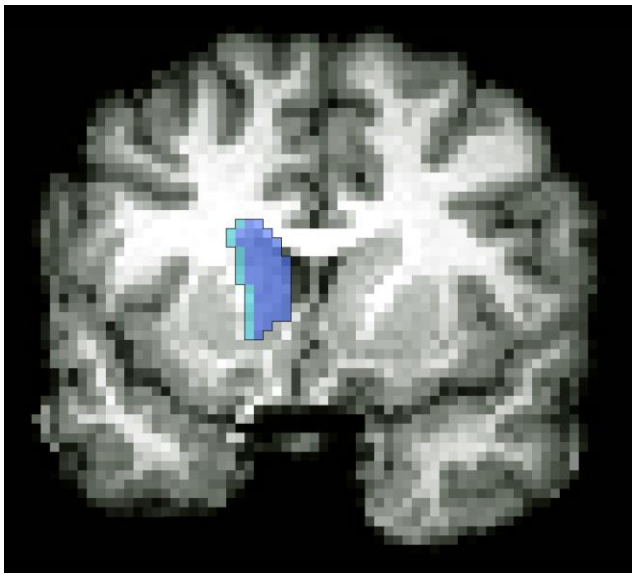

***Figure 5**. Coronal view of an ROI mask of the left hemisphere's caudate nucleus, on a T1-weighted image in 2mm^3 diffusion space. The lateral-most voxels are shaded in cyan. For a network to be considered a genuine representation of cortico-striatal circuitry, there must have been streamlines that passed the lateral-most voxels at some place along the length of the caudate nucleus.*

6.3.2 Cortico-thalamic/thalamo-cortical Circuitry

Streamlines with direct structural connectivity between the IFG and the ventral anterior nucleus of the thalamus were expected to lie within the anterior internal capsule and enter the thalamus at the capsular genu. Again, in the absence of unexpected structural anomalies or variance, networks could be expected to reliably bear resemblance across subjects and take a similar trajectory, if anatomically valid. A gross evaluation of the resulting pathways served to qualitatively characterize the trajectories of POr, PTr, and POp streamlines. Whether streamlines penetrated the proximal site of the ventral anterior nucleus and whether or not those streamlines appeared to pass through the internal medullary lamina to reach the pulvinar was recorded for all three frontal ROIs.

6.3.3 Intra-thalamic Integration/segregation of Cortical Networks

The degree to which cortico-thalamic/thalamo-cortical streamlines from different cortical regions overlapped within the thalamus was calculated to assess cortical integration/segregation. Specifically, the percentage of overlap for each possible set of two ROIs (i.e. POr/PTr, POr/POp, PTr/POp) was derived by dividing the volume of total thalamic voxels with cortico-thalamic/thalamo-cortical streamlines by the volume of voxels crossed by both pathways:

$$overlap_{ij} = \frac{N_{i \cap j}\ (V_{voxel})}{N_{i \cup j}\ (V_{voxel})},$$

where N is the number of thalamic voxels with streamlines from both ROIs ($i \cap j$), or the number of thalamic voxels with streamlines from either ROI ($i \cup j$), and V_{voxel} is the volume of a single voxel in mm^3. This fraction is simplified for clarity, however the values of both the numerator and the denominator were multiplied by V_{voxel} prior to extraction. This simple algorithm accounts for the size of the thalamus and thus is appropriate for group-level comparison of cortical integration/segregation in native space. Slight modification of this analysis method also enables quantification of topographical relationships among groups consisting of more than two cortical regions. However, additional analyses were not conducted for this dataset in consideration of the limited sample available for analysis with all three cortices ($N = 3$).

7 RESULTS

7.1 Cortico-striatal Circuitry

Results from networking cortico-striatal pathways are detailed in Table 1 (p. 45). Ford and colleagues' finding (Ford, Triplett, et al., 2013) of frontal streamlines projecting to the "anterior-superior third" of the putamen was replicable for all PTr networks (n = 11/11) and most POp networks (n = 7/11). These findings extended to the POr region as well, albeit less frequently (n = 5/11). Figure 6a depicts a 3D exemplar of this putaminal circuitry in a single subject.

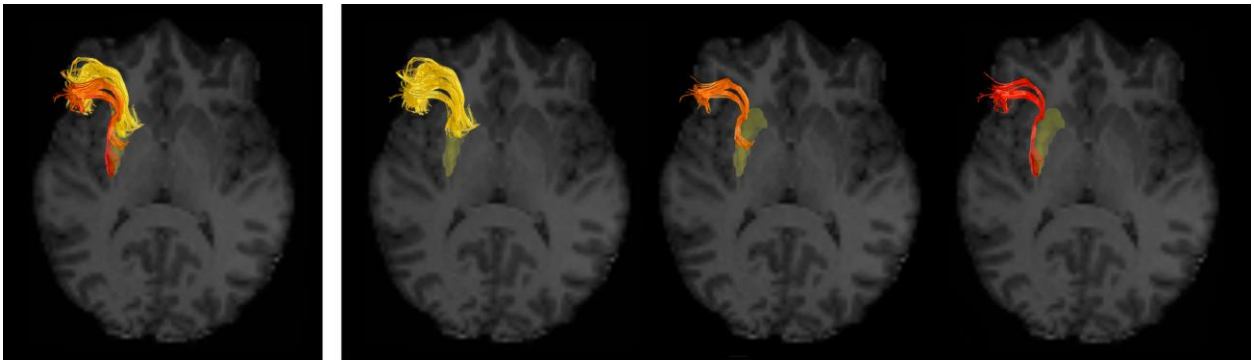

Figure 6. ***Intra-structural putaminal network for pars triangularis (PTr) in a single subject. Network filtering was used to visually distinguish between streamlines with entry at the anterior portion (a), midsection (b), and posterior end (c) of the putamen.***

Across cortical regions, two qualitatively distinct trajectories of unanticipated, co-occurring streamlines were regularly traced through the white matter lateral to the putamen. These streamline bundles entered the putamen laterally around either the more anterior portion of the midsection (Figure 6b), or towards the posterior of the putamen, respectively (Figure 6c). One subject's putaminal data (#2) only represented the lateral-most trajectory. (For clarity, this network is noted in Table 1 although it is not included in the sum of positive findings for the first aim.) Findings across subjects are depicted in a frequency map overlaid on a study-specific template in Figure 7. Although each of the three reported trajectories appeared visually distinct when rendered as streamline tractography files, some individual variation in placement was observed, comparably to that which was evident in the findings previously

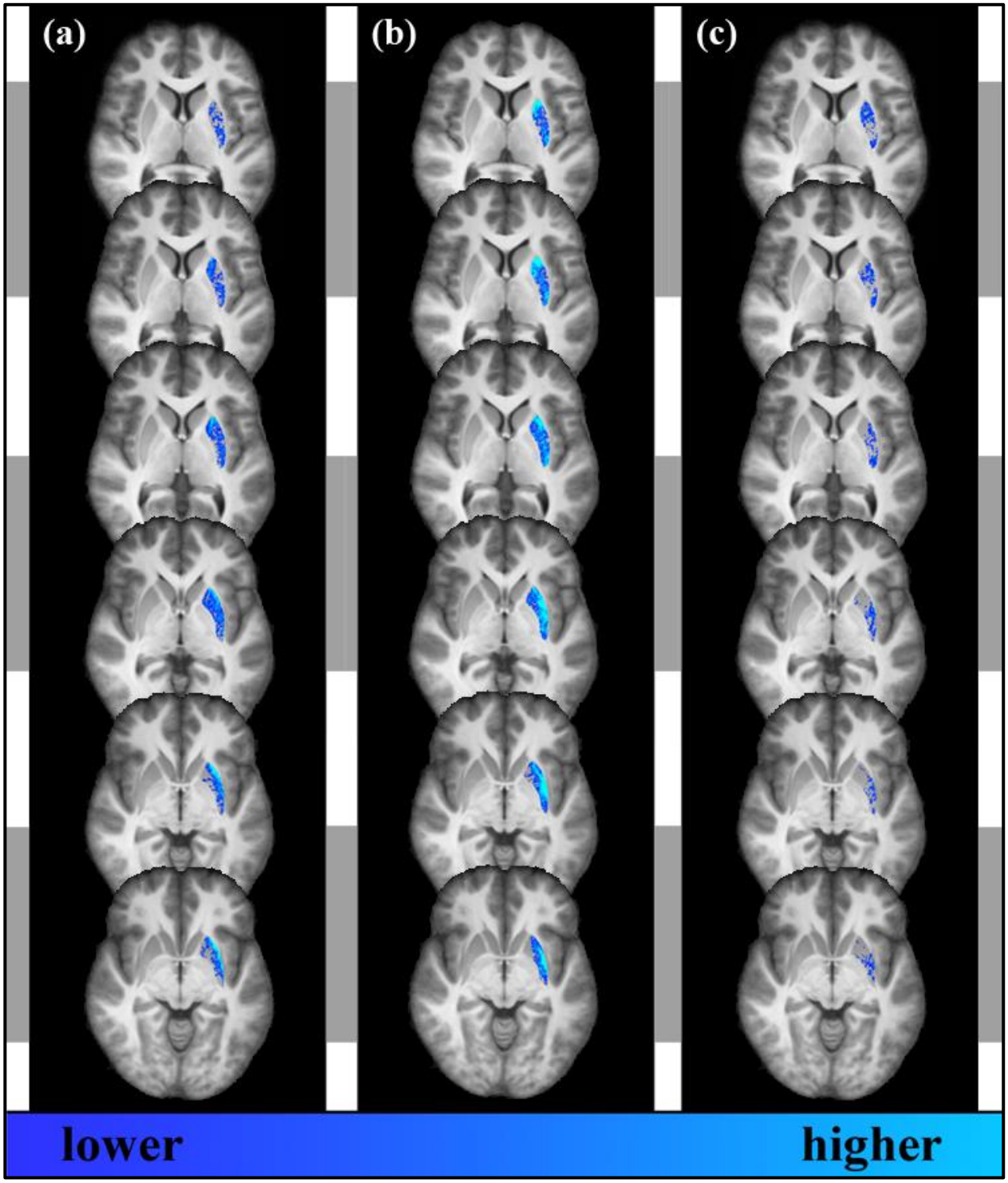

<u>Figure 7</u>. Frequency maps of intra-putaminal cortico-putaminal circuits from (a) pars orbitalis (POr), (b) pars triangularis (PTr), and (c) pars opercularis (POp), overlaid on axial slices of a 0.5mm3 resolution, study-specific template brain.

depicted by Ford, Triplett, and colleagues (2013). Thus, Figure 7 best represents the rostrocaudal and extensive nature of these findings, but also somewhat obscures the individual trajectories more readily visible in Figure 6. Nonetheless, the shift in frequency from the anterior-superior putamen to more posterior portions of the putamen, while descending ventrally through the depicted axial slices, can be seen relatively clearly.

Although the presence of putaminal connectivity via lateral white matter structures was not anticipated, these novel findings may be of consequence. Non-human, topographical research describing the subcortical brain's parallel, cortico-subcortico-cortical feedback loops detail fantastically complex distributions of variably dense, patchy, or banded putaminal axon terminations, which are organized along discrete medial-to-lateral and anterior-to-posterior gradients, with frontal circuits coursing through the internal and external capsules to reach their destination (e.g. Schilman, Uylings, Galis-de-Graaf, Joel, & Groenewegen, 2008; Whitworth et al., 1991). The three distinct streamline trajectories observed in this data might represent subsets of afferent cortico-striatal communication in humans, distributed along the rostrocaudal length of the putamen analogous to primate motor network circuitry.

The data produced from tracing striatal afferents to the caudate nucleus were mixed at best, consistent with previously documented attempts to analyze this subcortical structure with diffusion tractography (Ford, Triplett, et al., 2013). Due to a combination of overall network variability, limitations specific to this ROI, and more broadly applicable limitations (Section 8), positive results from this analysis (Table 1) are not reported with great confidence. In most cases, networks meeting the criteria described in Section 6.3.1 could not be traced (positive results for POr: n = 3/11; PTr: n = 7/11; POp: n = 5/11). Many networks contained a mix of streamlines that appeared to be exclusively capsular, possibly represented connectivity with the caudolenticular grey bridges, may have reflected genuine circuitry, and/or seemed to have realistic initial trajectories coupled with termination points along the ventricles. A subset of the observed null streamlines behaved as described previously by Ford and colleagues, approaching the surface of the caudate nucleus en route to the thalamus. A portion of these mixed findings may simply represent ROI dilation during the co-registration process. Thus, individual

subcortical ROI refinement after co-registration might have prevented the inclusion of some of these streamlines. As noted in Section 6.2.5, exclusionary regions were manually drawn on diffusion-weighted images, and networks confined to regions of possible ROI dilation or volume averaging were not reported as positive findings for any of this thesis' analyses. For this reason, ROI dilation accounted for a degree of qualitative variance, but did not contribute to reported network counts or null findings.

Streamline trajectories that appeared qualitatively reasonable entered the caudate nucleus in the head and/or body of the structure, as initially predicted. Figure 8 depicts robust POr and PTr network exemplars of this circuitry, which appear to be harmonious with Alexander, Crutcher, and DeLong's (1990) description of primate dorsolateral frontal afferents that terminate in the caudatal head and along a "continuous rostrocaudal expanse that extends to the tail of the caudate". Note that the anatomical underlay of Figure 8 is opaque so streamlines anterior/posterior or medial/lateral to the visual plane can be readily seen. Cortical ROIs and the caudate nucleus ROI are represented by orange and blue shapes, respectively. In multiple datasets, caudatal networks appeared to lie along an initially "realistic" trajectory that entered the caudate nucleus in the head/body region as anticipated, but ultimately looped back anteriorly as if following the flow of cerebrospinal fluid (CSF) through the ventricular space (Greitz, Franck, & Nordell, 1993), indicating some degree of "CSF contamination". The POp network shown in Figure 8 takes this trajectory along the ventricles. Please note that ventricular alignment was determined with 3D data interaction, but could not be shown canonically in a static image. Other networks depicted in Figure 8 did not appear to lie along the ventricles when similarly manipulated with track file viewing software.

The occurrence of CSF contamination highlights imaging obstacles specific to the caudate nucleus, relative to this investigation's other ROIs, and indicates a high likelihood that ventricular masking to decrease false-positives at the post-processing phase would eliminate many true-positive axonal representations as well. Evidence of CSF contamination further suggests the possibility that exclusion of fibers crossing the mid-sagittal slice (see Section 6.2.5) might have eliminated streamlines containing subsets of true-positive data. In future studies, this limitation could be accounted for on the

front-end somewhat easily by eliminating the ventricles from the brain mask used to generate global tractography files. Alternatively, free-water elimination (FWE) models have been proposed for globally reducing confounds related to isotropic diffusion (e.g. Hoy, Kecskemeti, & Alexander, 2015). However,

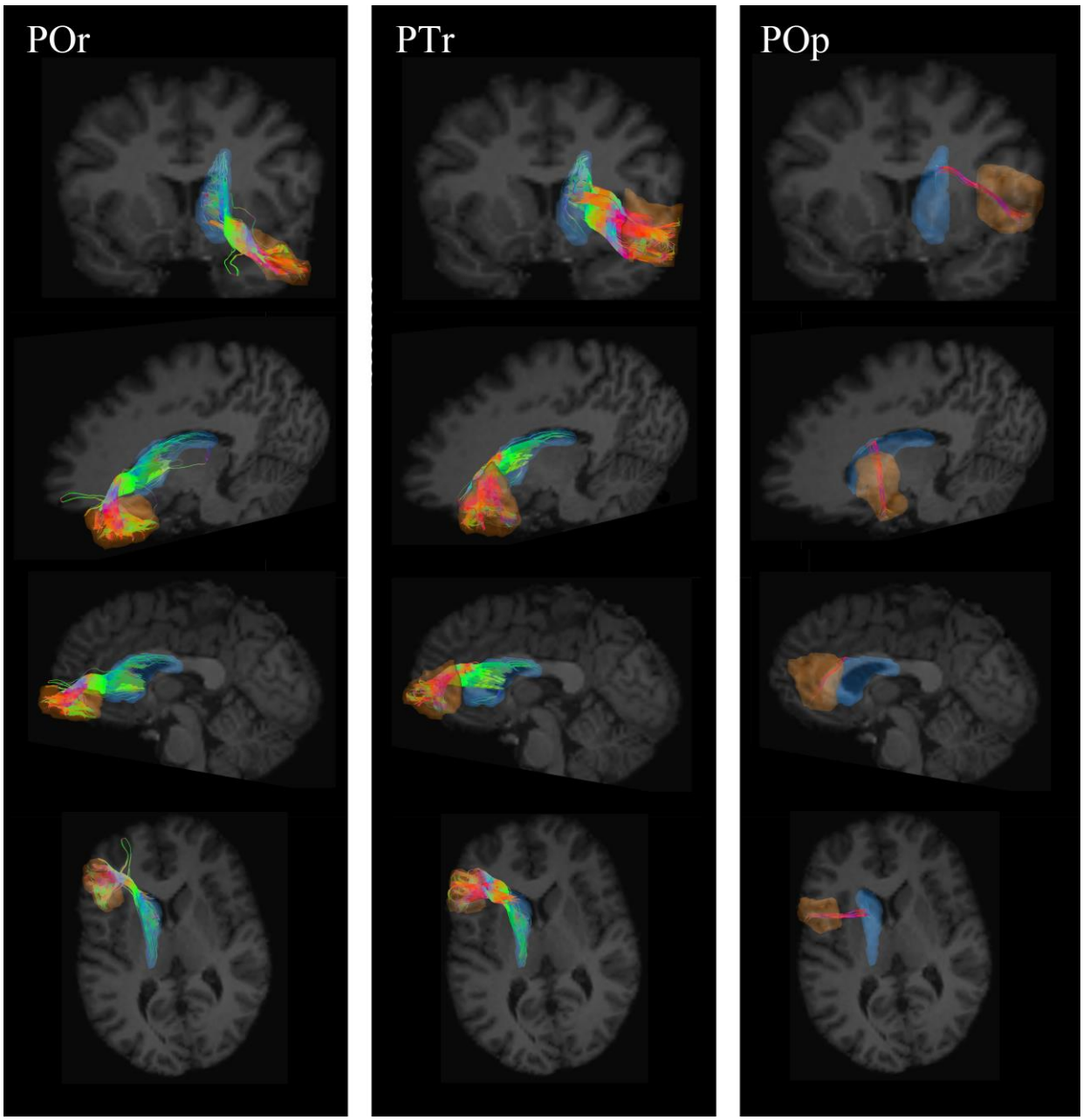

Figure 8. ***Intra-structural caudate nucleus networks for pars orbitalis (POr), pars triangularis (PTr), and pars opercularis (POp) in a single subject.***

FWE solutions may also introduce novel confounds in regions devoid of isotropy and requires a multi-shell acquisition. The bottom line is that accounting for the ventricles in some manner is strongly suggested for future investigation of intra-structural tractography of the caudate nucleus. Precise, conservative refinement of caudate nucleus segmentations after co-registration may have also decreased network variability in this dataset. Other optimizations suggested by this thesis' results primarily relate to acquisition parameters, and are discussed more broadly as they apply to all three aims (see Section 8).

7.2 Cortico-thalamic/thalamo-cortical Circuitry

Consistent with the striatal findings described in the previous section, it was not possible to trace cortico-thalamic/thalamo-cortical fibers from all regions for all subjects. Only PTr projections to/from the thalamus could be traced in 11/11 subjects. In contrast, cortico-thalamic/thalamo-cortical projections of POr and POp were traceable in 6/11 or 5/11 subjects, respectively. Individual subject results are detailed in Table 2 at the end of this section (p. 46). Track data contained streamlines that passed through the internal capsule to reach the proximal site of the ventral anterior nucleus at the capsular genu, in all instances for which cortico-thalamic/thalamo-cortico networks could be traced. With one exception, streamlines took a qualitatively similar trajectory through the internal medullary lamina, with streamlines terminating/originating in the pulvinar. This circuitry is depicted in 3D for a representative subject in Figure 9, and with 2D frequency maps for each cortical region in Figure 10. Frequency maps are overlaid on a normalized, $0.5mm^3$ resolution, study-specific template brain for display purposes. Streamline terminations/origins in the mediodorsal nucleus and/or intralaminar nuclei appeared to be typical as well, consistent with established primate literature and suggesting an avenue for future, intra-thalamic tractography research with segmented thalamic nuclei or end-point visualizations (Goldman-Rakic & Porrino, 1985; Sadikot & Rymar, 2009).

The one thalamic network that did not reach the pulvinar was a PTr network that concluded its run in the ventral anterior nucleus. This network was traced from a subject notable for considerable head tilt of yaw misalignment in the MRI scanner. This subject was not initially excluded from analysis on the basis that frontal susceptibility artifacts did not result in clear IFG signal loss in either hemisphere.

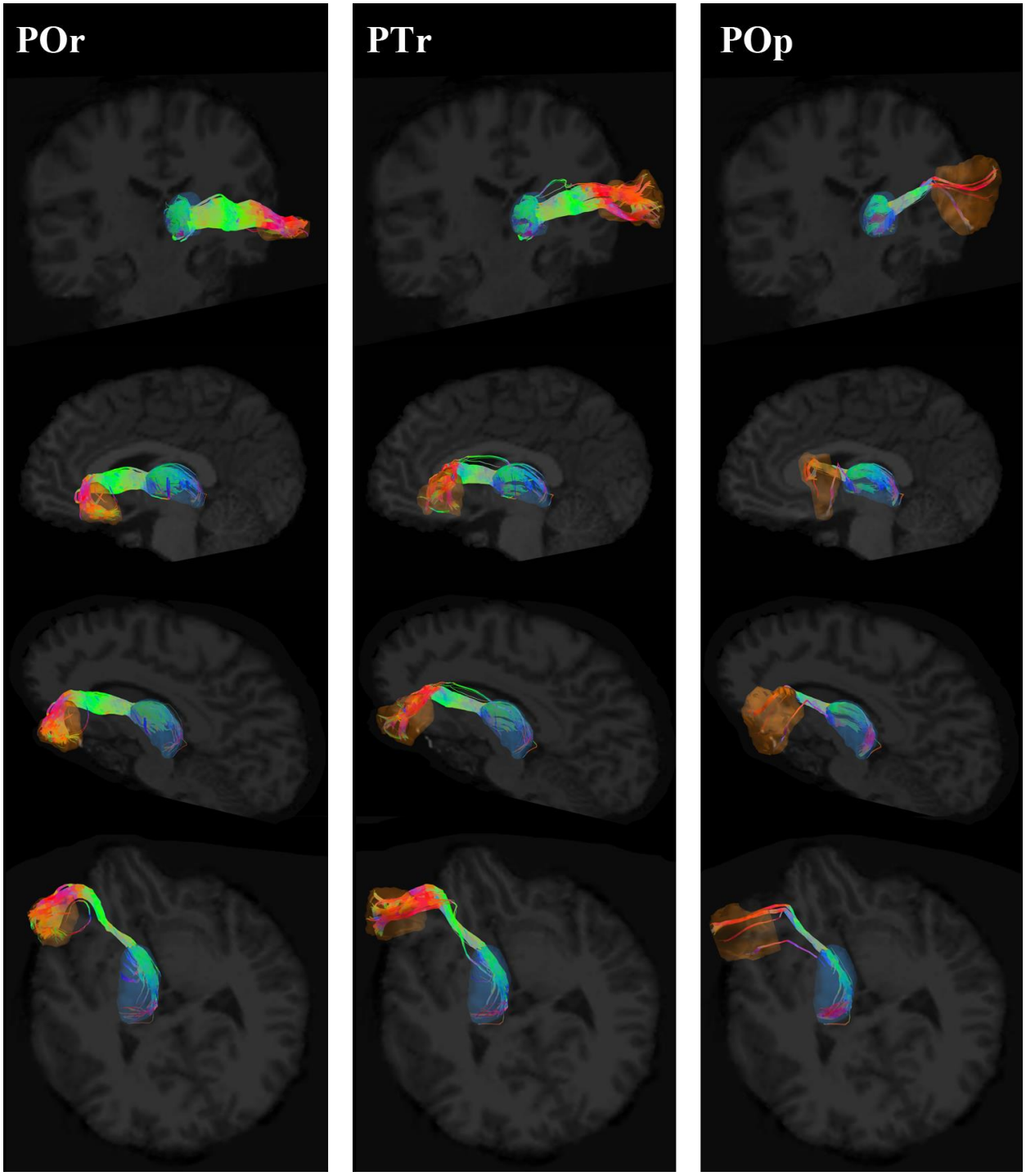

<u>Figure 9</u>. Intra-structural thalamic networks for pars orbitalis (POr), pars triangularis (PTr), and pars opercularis (POp) in a single subject.

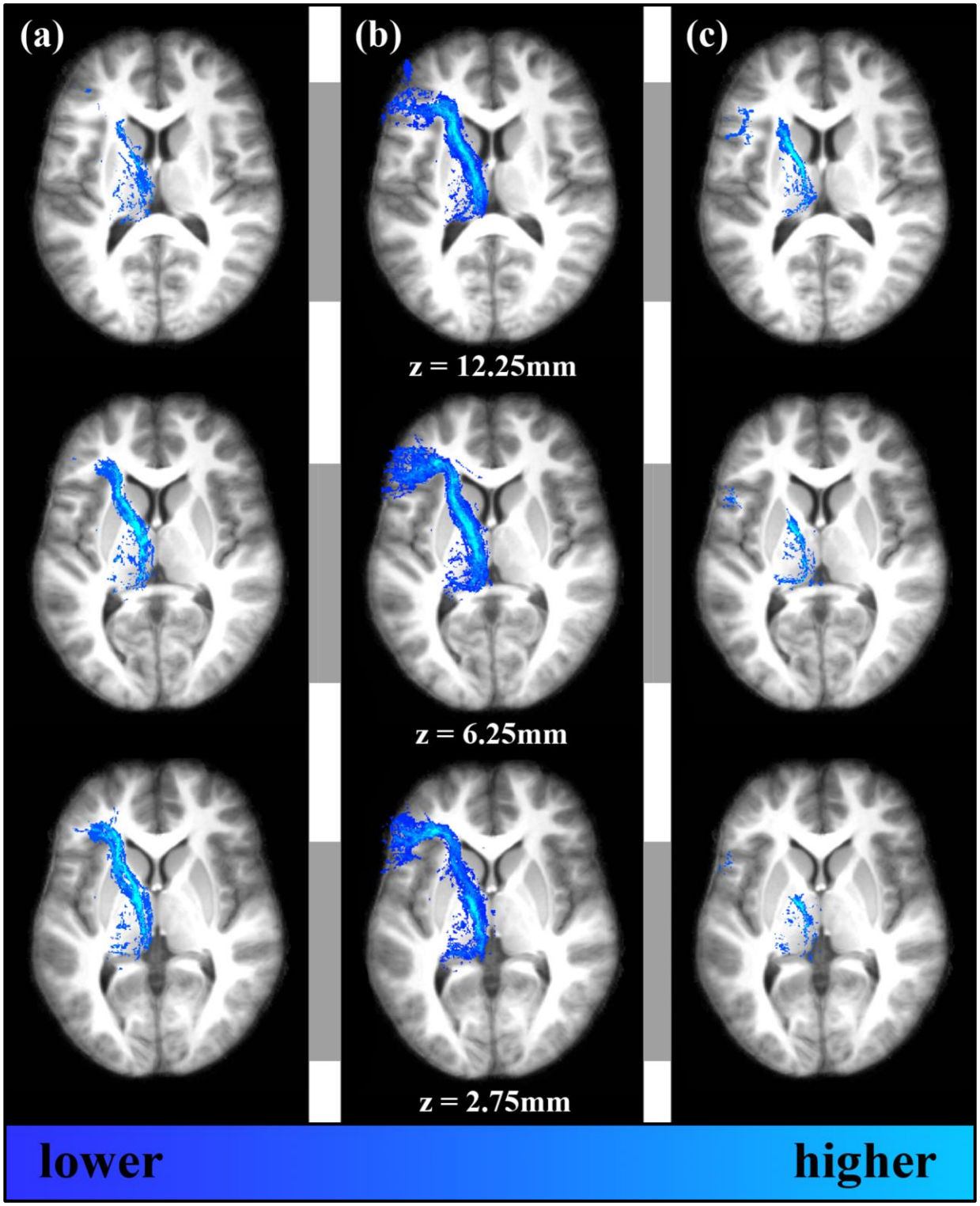

<u>Figure 10</u>. Frequency maps of thalamo-cortical/cortico-thalamic circuits from (a) pars orbitalis (POr), (b) pars triangularis (PTr), and (c) pars opercularis (POp), overlaid on three axial slices of a 0.5mm^3 resolution, study-specific template brain.

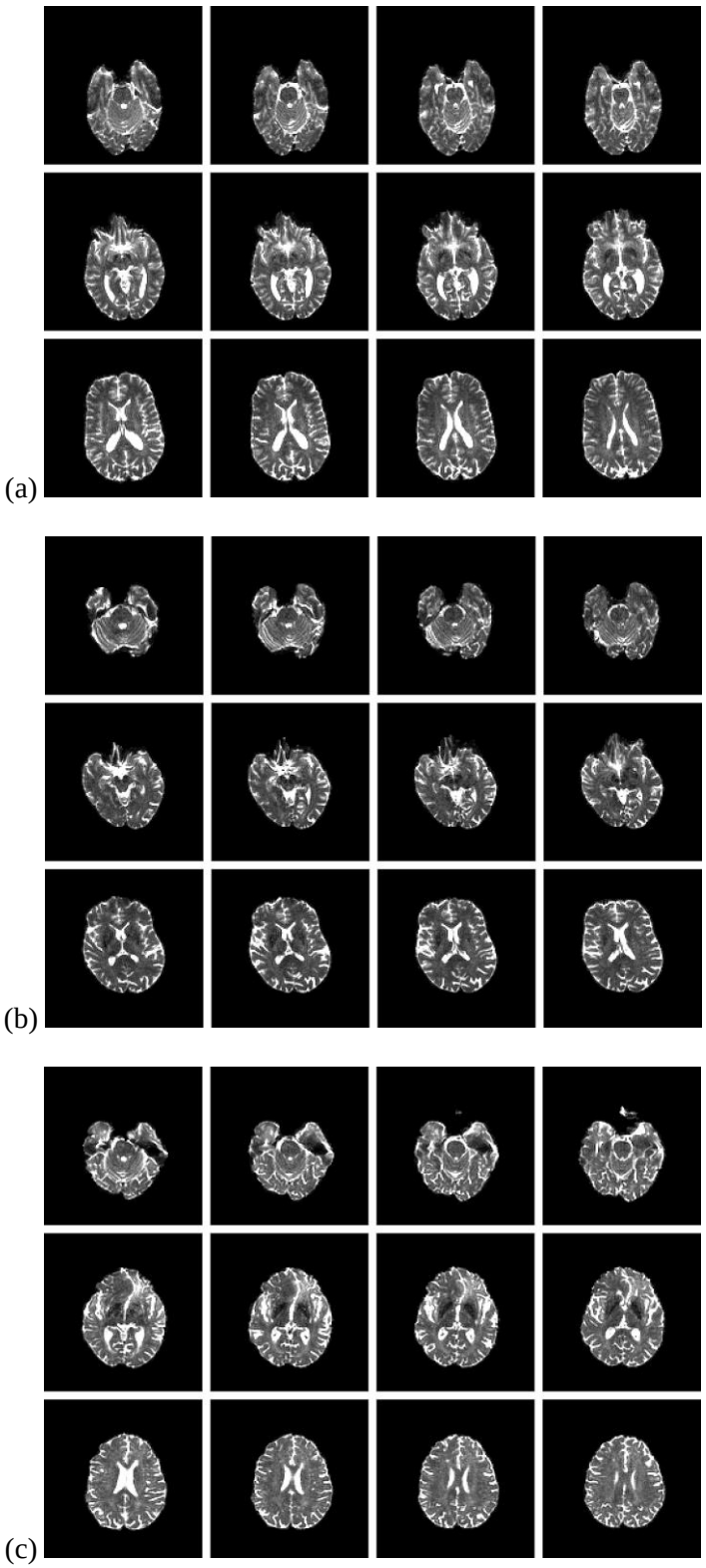

<u>Figure 11</u>. Asymmetries in DWI scans acquired (a) anterior-to-posterior with yaw head tilt, (b) anterior-to-posterior with roll and yaw head tilt, and (c) right-to-left.

Nonetheless, head misalignment could presumably result in asymmetry of EPI artifacts that would affect data across networks, similarly to the asymmetry seen with diffusion-weighted images acquired along the right-to-left phase encode direction, although at a lesser magnitude. To demonstrate this for consideration, un-weighted diffusion scans from this subject (#7), a subject from another dataset representing dual roll and yaw head tilt, and a subject acquired with right-to-left phase encoding are depicted in Figure 11. Indeed, findings for subject #7 were notably sparse. Out of nine possible networks (3 cortical ROIs x 3 subcortical ROIs), only 3/9 networks could be traced. In all three of these networks, trajectories qualitatively consistent with other subjects' data and replicated research were accompanied by suspect variance suggesting questionable data quality. That said, co-occurrence of reasonable findings with false-positives was not entirely unique to this subject, and structural connectivity with the ventral anterior nucleus was expected independent of pulvinar connectivity. For this reason, this subject's positive results were reported as valid.

7.3 Intra-thalamic Integration/segregation of Cortical Networks

Evaluation of intra-thalamic cortical network integration/segregation was possible for eight subjects, with 14 groups total for comparison (POr/PTr, n = 6; PTr/POp, n = 5; POr/POp, n = 3). Individual subject results, composite means, and standard deviations of overlap values for each network group are listed in Table 3 (p. 47). The primary analysis was complimented by an exploratory, native-space analysis in an otherwise identical, 0.5mm^3 Cartesian coordinate plane to evaluate streamline data at a higher resolution than is possible with 2mm^3 voxels. Results from both analyses are reported for the purpose of discussing potential future directions for application of this thesis' methodology, however description of the 0.5mm^3 analysis is limited to Appendix C in consideration of experimental use of the tractography file format.

Predominance of cortico-thalamic/thalamo-cortical circuitry overlap was greatest for the POr/PTr group (mean = 51.25%; n = 6), but indicated largely segregated, intra-thalamic cortical circuits. Comparison of PTr/POp similarly revealed a trend towards segregation of network circuits (mean = 49.96%; n = 5). In contrast with the degree of overlap demonstrated by the POr/PTr and PTr/POp groups,

less overlap of intra-thalamic circuits was observed for the POr/POp group (mean = 32.90%; *n* = 3). Of note, greater proportions of overlap were evident in groups of gyral regions that consistently share physical boundaries and tend to activate during similar cognitive tasks (i.e. POr/PTr and PTr/POp; reviewed in Sections 2.1 and 2.1.2). Overall, findings were consistent with the hypothesis that cortical circuits are primarily segregated within the thalamus, with possible integration along borders. Figure 12 depicts this pattern in a single subject (#10), prior to masking voxels outside the thalamus for quantitative comparison.

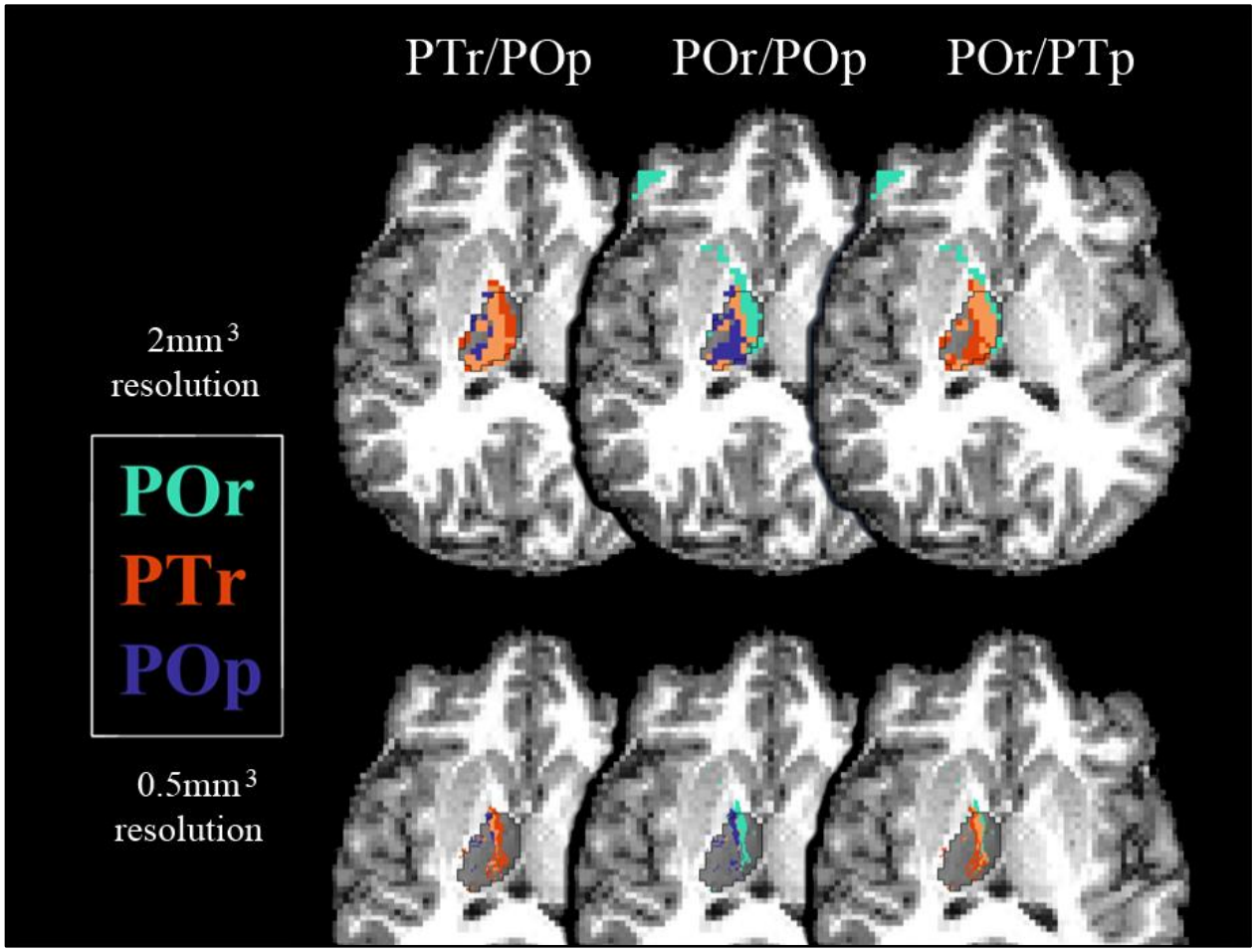

***Figure 12**. Native-space exemplar of intra-thalamic, cortical networks of pars orbitalis (POr), pars triangularis (PTr), and pars opercularis (POp) in a single subject. Structural network overlap is depicted in light orange. Images are overlaid on a 2mm^3 resolution T1-weighted image.*

Table 1. Cortico-striatal structural networks

Subject		**Putamen**	**Caudate Nucleus**	*Both Structures*
1	POr			
	PTr	✓		
	POp	✓	✓	✓
2	POr	□□□✓□□	✓	□□□✓□□
	PTr	✓	✓	✓
	POp			
3	POr	✓		
	PTr	✓		
	POp			
4	POr	✓		
	PTr	✓	✓	✓
	POp	✓		
5	POr			
	PTr	✓	✓	✓
	POp	✓	✓	✓
6	POr	✓		
	PTr	✓	✓	✓
	POp		✓	
7	POr			
	PTr	✓		
	POp	✓		
8	POr			
	PTr	✓	✓	✓
	POp	✓	✓	✓
9	POr	✓	✓	✓
	PTr	✓		
	POp	✓		
10	POr	✓	✓	✓
	PTr	✓	✓	✓
	POp	✓	✓	✓
11	POr			
	PTr	✓	✓	✓
	POp			
n	*POr*	5	3	***23 (putamen)***
	PTr	11	6	***14 (caudate)***
	POp	7	5	

Abbreviations: pars orbitalis (POr), pars triangularis (PTr), pars opercularis (POp).
** Network circuitry could be traced, however no putaminal circuitry took the hypothesized trajectory.*

Table 2. Cortico-thalamic/thalamo-cortical structural networks

Subject		**VA Nucleus**	**Pulvinar Nucleus**	*Both Nuclei*
1	POr			
	PTr	✓	✓	✓
	POp	✓	✓	✓
2	POr	✓	✓	✓
	PTr	✓	✓	✓
	POp			
3	POr	✓	✓	✓
	PTr	✓	✓	✓
	POp			
4	POr	✓	✓	✓
	PTr	✓	✓	✓
	POp			
5	POr			
	PTr	✓	✓	✓
	POp	✓	✓	✓
6	POr			
	PTr	✓	✓	✓
	POp			
7	POr			
	PTr	✓		
	POp			
8	POr	✓	✓	✓
	PTr	✓	✓	✓
	POp	✓	✓	✓
9	POr	✓	✓	✓
	PTr	✓	✓	✓
	POp	✓	✓	✓
10	POr	✓	✓	✓
	PTr	✓	✓	✓
	POp	✓	✓	✓
11	POr			
	PTr	✓	✓	✓
	POp			
n	*POr*	6	6	
	PTr	11	10	***22 (total)***
	POp	5	5	

Abbreviations: ventral anterior (VA), pars orbitalis (POr), pars triangularis (PTr), pars opercularis (POp).

Table 3. Percentage of intra-thalamic overlap for cortico-thalamic/thalamo-cortical circuits

	based on 2mm³ voxels			*based on 0.5mm³ voxels*		
Subject	POr/PTr	POr/POp	PTr/POp	POr/PTr	POr/POp	PTr/POp
1	*N/A*	*N/A*	**56.04**	*N/A*	*N/A*	**29.55**
2	**46.82**	*N/A*	*N/A*	**29.96**	*N/A*	*N/A*
3	**46.82**	*N/A*	*N/A*	**9.21**	*N/A*	*N/A*
4	**28.48**	*N/A*	*N/A*	**12.97**	*N/A*	*N/A*
5	*N/A*	*N/A*	**47.26**	*N/A*	*N/A*	**17.88**
6	*N/A*	*N/A*	*N/A*	*N/A*	*N/A*	*N/A*
7	*N/A*	*N/A*	*N/A*	*N/A*	*N/A*	*N/A*
8	**51.63**	**9.23**	**23.12**	**25.76**	**1.22**	**2.33**
9	**71.74**	**54.39**	**59.69**	**50.35**	**15.55**	**20.28**
10	**46.41**	**35.07**	**63.71**	**22.81**	**14.73**	**33.73**
11	*N/A*	*N/A*	*N/A*	*N/A*	*N/A*	*N/A*
n	6	3	5			
Mean	51.26	32.90	49.96	25.18	10.50	20.75
SD	14.88	22.65	16.19	14.61	8.05	12.18

Abbreviations: pars orbitalis (POr), pars triangularis (PTr), pars opercularis (POp).
Note. Shaded cells represent data generated from the primary analysis.

8 STRENGTHS AND LIMITATIONS

Acknowledging the limitations of this dataset along with this thesis' methodological strengths is crucial for interpretation of networking results. It's plausible that the ability to trace cortico-striatal fiber bundles (e.g. the unanticipated putaminal pathways) that were not detected in previous investigations (e.g. Ford, Triplett, et al., 2013) was an opportune product of the methodological innovations used for network tracking. Ongoing, pilot work comparing this thesis' methods to previously validated pipelines appears to

indicate that direct, intra-structural networking results in more comprehensive and robust circuitry representations. It is likely that this contrast is due to decreased sensitivity loss at the networking phase of processing, as this thesis' methodological innovations do not affect global fiber estimation or alter individual streamline data in any way prior to direct networking. Intra-structural networking also enabled visualization and quantification of estimated fibers at a level previously unattainable without sacrificing specificity (e.g. without direct networking or within a probabilistic framework).

However, suspected false-positive streamlines were sometimes observed in this dataset. For instance, individual streamlines occasionally passed through the putamen and terminated in the globus pallidus. Similar false-positives were not encountered by Ford and colleagues (Ford, Triplett, et al., 2013), who searched for pathways between PTr/POp and the globus pallidus in half of their subjects (5/10), but reported no instances of false-positive findings. It is also plausible that some streamlines eliminated with striatal exclusion masks during processing may have reflected multi-fiber cortical pathways between the putamen and caudate nucleus via the caudolenticular grey bridges (Whitworth et al., 1991), in addition to fibers simply resulting from ROI dilation after co-registration. Although this thesis' methodological innovations appear to improve network filtering, producing true-positive data still heavily relies on the assumption of high-integrity global fiber estimation prior to networking. Thus, false-positive results in this dataset may indicate that the global tracing algorithm was not always successful at differentiating between neurons with synaptic association or within complex fiber junctions.

Structural connectivity results that do not replicate previously substantiated findings should be approached with caution unless successfully replicated in other datasets, in light of indications of suboptimal MRI data. That withstanding, the semblance of POr fibers as compared to those of classical Broca's area, the relative consistency of the unanticipated putaminal fiber trajectories across cortical regions, and robust findings for replicated putaminal/thalamic fiber networks collectively imply a predominance of true-positive findings among less-prevalent false-positives. As with any neuroimaging research, specific inquiry based on substantiated, anatomical expectations should accompany interpretation of results, both promising and otherwise. In this dataset, most results that were not null

appeared to be highly consistent with neuroanatomical expectations based on previous human and non-human research, thus lending confidence to this research as a successful replication and launching point for more detailed investigations of subcortical circuitry. However, given the possibility of erroneous over-tracking of multi-fiber connections, future replication with *a priori* anatomical questions is critical. In particular, the posterior-most, lateral putaminal trajectory would benefit from comparison to neighboring claustral pathways. Prior research in humans and primates has demonstrated cortico-claustral connectivity as well as claustro-putaminal connectivity (Milardi et al., 2013; Reser et al., 2014). Due to the positioning of these claustral pathways and potential volume averaging in the narrow region between the putamen and the claustrum, if multi-synaptic claustral pathways linking the cortex to the putamen were overtracked in this dataset, these erroneous findings might reasonably present with some regularity across subjects. As an alternative to network comparisons in future studies, precise and well-defined claustrum exclusion masks might allow for eliminating streamlines that represent overtracked, multi-synaptic claustral projections.

As a point of emphasis, data produced for the caudate nucleus may reflect true-positive findings of structural connectivity and/or a step forward towards unmasking them, but as a whole are questionable as evidence of the ability to estimate or trace caudatal white matter relationships using *in vivo* diffusion tractography. In many ways, this thesis' findings best represent a dissociation of methodological effectiveness for tractography of the caudate nucleus relative to other subcortical regions, while highlighting some of the possible pitfalls worth avoiding proactively. As noted previously, accounting for the lateral ventricles is critical and should occur prior to global fiber estimation to avoid tracing false streamlines. Future methodological advancement might ultimately lessen the impact of ventricular fluid momentum, however in any case it would be advisable to simply eliminate this confound instead of relying on complex algorithms to render it obsolete.

Single-shell DWI acquisition may have contributed to both null and false-positive findings, beyond but inclusive of the caudate nucleus. Diffusion gradients were applied as a single shell (i.e. weighted b-value) along one phase-encoding direction. Multi-shell DWI data is inherently preferable to single-shell DWI data, as the magnetic resonance (MR) signal of a given voxel recorded during

acquisition is a joint function of the strength of the gradient pulse manipulated to achieve a particular b-value and the underlying microstructure of the tissue (Assemlal, Tschumperlé, Brun, & Siddiki, 2011), among other factors. Thus, programmed variations in gradient strength will heterogeneously affect signal based on the features of the tissue. A set of data with sensitivity to a broader range of tissue types should inherently increase the integrity of the tensor distribution fit from MR signal attenuation for angular reconstruction, while also helping to differentiate actual brain tissue from CSF.

Both of the previous subcortical tractography investigations upon which this thesis' methods were based (Bohsali et al., 2015; Ford, Triplett, et al., 2013), in addition to other relevant research produced by members of this research group (Colon-Perez, Spindler, et al., 2015; Colon-Perez, Triplett, et al., 2015; Ford, Colon-Perez, et al., 2013), used a two-shell acquisition scheme for data collection (n = 6, b = 100 s/mm^2; n = 64, b = 1000 s/mm^2). The addition of these low-strength gradients may have increased the integrity of fit for high sensitivity global fiber estimation. Indeed, Bohsali et al. reported substantially larger global tractography file sizes of up to ~1/4 TB, reflecting a greater number of estimated neural axons. Global tractography data from this thesis averaged 14.09 GB per file (SD = 1.14 GB).

Consistent with the results of this investigation, Bohsali and colleagues (Bohsali et al., 2015; Ford, Triplett, et al., 2013) reported more robust data from PTr networks than POp networks, based on the within-network volumes of voxels occupied by streamlines (i.e. "track volume"). This pattern applied to subcortical ROIs across studies, including the putamen, the thalamus, and individual masks of the thalamus' ventral anterior and pulvinar nuclei. However, these researchers reported successfully tracing networks in all of their subjects for both PTr and POp (N = 10). In spite of observed sensitivity increases resulting from methodological innovation, the present study reflected comparable success for putaminal and thalamic circuits of the PTr region only (PTr = 100%, n = 11; POp = 45-64%, n = 5-7; POr = 45-55%, n = 5-6). Conceivably, results across aims may have been more robust had additional shells been collected for increasing the integrity of MR signal attenuation modeling.

Several *post-hoc* analyses were performed to empirically investigate other potential sources of contrast in networking success between the present study and previous investigations (Appendix D). In

summary of these inquiries, differences in seed density did not appear to explain a sufficient portion of variance to account for null findings and a more liberal angular deviation threshold likely would have increased the prevalence of false-positive data. More closely mimicking the methodologies used by Bohsali et al. (2015) and Ford, Triplett, et al. (2013) for direct, between-region networking generated qualitatively similar albeit less robust networks, while resulting in complete inability to trace POr network streamlines. It is posited that methodological innovation necessarily improved sensitivity to POr fibers, while acquisition-related factors such as the use of single-shell data to model the MR signal may have negatively impacted the integrity of both POr and POp tracings. Subject-specific variables including age, gender, and cortical ROI size were additionally explored, but differences did not appear to correlate with structural connectivity results.

Interpreting the source of null POr findings relative to null POp findings requires more specific consideration of each regions' imaging obstacles. For purposes of comparison, there was no baseline data regarding POr's subcortical connectivity against which to compare the current findings. Diffusion-space POr ROIs were exceptionally smaller in all subjects, decreasing the overall number of seeds from which streamlines were propagated, while perhaps increasing the proportional prevalence of deleterious volume averaging at regional boundaries (POr volume rounded mean = 2826 mm^3; PTr = 7908 mm^3; POp = 9716 mm^3). The angulation of POp fibers passing the circular sulcus to approach or traverse the internal capsule is necessarily more pronounced than that of POr (or PTr), theoretically presenting the latter an advantage for *in vivo* fiber estimation. However, POr is also disadvantageously located within or adjacent to orbitofrontal signal loss and susceptibility artifacts notoriously common with EPI acquisitions, moderated by phase-encoding direction (De Panfilis & Schwarzbauer, 2005), and evident in this dataset. Generally speaking, given an optimal imaging protocol it is possible to partially correct susceptibility artifacts by computing an estimated field of global distortion from reverse phase-encoded acquisitions (Andersson, Skare, & Ashburner, 2003; Andersson & Sotiropoulos, 2016). Because volumes of only a single phase-encoding direction were acquired, preprocessing could not eliminate this EPI artifact. Of note, data for the prior research cited for tractography of Broca's area's subcortical connectivity (Bohsali

et al., 2015; Ford, Triplett, et al., 2013) was also acquired along a single phase-encoding direction, however, these data were acquired in the opposite direction (i.e. posterior-to-anterior). It is additionally worth noting that milder susceptibility artifacts introduced by the lateral ventricles could theoretically also influence caudate nucleus fiber estimations, in addition to the discussed caudate-specific imaging considerations. Advanced susceptibility artifact correction in an optimal dataset might therefore benefit caudate nucleus tractography as well as POr networking.

In summary, the particular vulnerabilities of POr and POp should be given weight when interpreting null structural connectivity findings from this thesis and when designing imaging paradigms. Null findings absent from prior, relevant studies may reflect less sensitive fiber estimation per this investigation's use of single-shell DWI data for signal attenuation modeling and fiber reconstruction. Although most reported, positive findings appear to be anatomically reasonable, replication is necessary to rule out representation of overtracked, multi-fiber pathways.

Limitations more generally inherent to all contemporary DWI analyses, such as inability to determine directionality of information transfer along axonal representations, also apply to this research. Because head tilt in the scanner was not controlled for during acquisition, confounds related to head tilt might have had the potential to affect data integrity. Forty-five percent (45%) of data acquired with this archival dataset had to be excluded due to atypical white matter atrophy, radiologically evident medical conditions, head placement outside the MRI scanner field-of-view, or motion, which DWI is notably sensitive to. A larger sample size would have been ideal, particularly given the novel methodological goals of this research. Reported results are intended as a healthy, baseline description and cannot be generalized beyond English-speaking, young adult populations. Finally, as concluding remarks, the cumulative obstacles presented by this dataset's limitations were undeniably substantial. Without the sensitivity increases introduced by this thesis' networking innovations, at least 22% of the reported networks across aims would have presented as false-negative results. In other words, roughly a quarter of this thesis' reportable data would have been overlooked without methodological optimization.

9 DISCUSSION

This research used high-angular deterministic tractography to replicate previous findings of classical Broca's area's direct, subcortical, structural connectivity and extend them to include pars orbitalis (POr), the lesser-studied region of the inferior frontal gyrus (IFG). Thalamic connectivity to/from the cortex passed through the ventral anterior nucleus of the thalamus at the genu of the internal capsule and extended into the pulvinar nucleus, an area of reciprocal connectivity with the temporal, parietal, and occipital lobes. This convergence of white matter in the pulvinar might enable efficient coordination amongst cerebral lobes and the sharpening of attention on salient information for multi-modal integration of neurolinguistic processes. Pulvinar-driven processing might also work in collaboration with domain-general, striatal influences moderated by the cortices to support integration of verbal information for speech output and comprehension. This thesis' thalamic findings, depicted in Figures 9 and 10, replicate previous research illustrating fronto-pulvinar and intra-thalamic connectivity *in vivo* in humans (Bohsali et al., 2015; Nishio et al., 2014), and demonstrate agreement with *ex vivo* tracing research in macaques (Asanuma et al., 1985; Goldman-Rakic & Porrino, 1985; Romanski et al., 1997). Additional figures depicting these results can be found in Appendix D. Evidence for direct structural connectivity with the thalamus was particularly strong for pars triangularis (PTr), and observed in pars opercularis (POp) and POr as well (Table 2). Broadly, these findings contribute to evidence that classical Broca's area's thalamic circuitry can be elucidated with *in vivo* diffusion tractography, while suggesting a substrate through which POr could subcortically modulate linguistic processes driven by the language network.

Both the putamen and the caudate nucleus, component structures of the neostriatum, are known to be densely interconnected with the thalamus and neocortex via series of complex, parallel circuitry loops. Subcortically, the striatum may assist the thalamus with accurate and efficient word selection by increasing the signal-to-noise ratio of accurate word choices among alternatives (Crosson, 2013). Direct cortical projections to the striatum, believed to primarily operate on domain-general language functions, were examined for this thesis and found to approach the internal capsule. Broadly, this circuitry has been posited to contribute to language faculties by supporting contextually-bound lexico-semantic and

syntactic unification (Dominey et al., 2009; Hinaut & Dominey, 2013), select aspects of syntactic processing (Kotz et al., 2003; Teichman et al., 2015), and verbal learning (Ullman, 2016).

This thesis' investigation of cortico-putaminal connectivity replicated previous findings for classical Broca's area (Figure 6a) while extending them to POr, implying that POr may be poised to contribute to language cognition via cortico-putaminal circuitry. In harmony with thalamic findings and previous investigations (Bohsali et al., 2015; Ford, Triplett, et al., 2013), evidence of striatal structural connectivity was most robust for the PTr region, but observed in a number of cases for POp and POr as well (Table 1). Two lateral trajectories to more posterior regions of the putamen were also revealed by this investigation, across IFG cortices (Figure 6b-c). These fiber bundles appeared to diverge from or pass the internal capsule to reach the putamen via the external capsule, entering the midsection or posterior region of the putamen laterally. Connectivity with the caudate nucleus was also observed, but due to preponderance of variability cannot be confidently inferred and will not be discussed further.

Fiber estimations terminating in the mid-to-posterior putamen were not anticipated, in consideration of primate research highlighting the putamen as a specialized center of primarily motor and sensory activity, divergently associated with higher-order cognition in its rostral-most aspects only. However, the notion that humans might exhibit structural connectivity patterns that do not entirely correspond with those of primates or other species is reasonable, particularly for the language network. Striatal connectivity patterns are observed to differ among mammalian motor networks, with regards to connectivity localization although not general somatotopic representation (reviewed by Whitworth et al., 1991). Broadly, primate motor/sensory putaminal afferents are organized both anteriorly-to-posteriorly and laterally-to-medially, consisting of fine interdigiated bands of terminals from non-adjacent cortices, regions of gross terminal segregation, and overall diffuse but patchy distribution (Selemon & Goldman-Rakic, 1985). In both rats and primates, external capsule fibers such as those observed with this investigation have been reported, although not for IFG regions (e.g. Schilman et al., 2008; Whitworth et al., 1991).

Presuming the authenticity of the fibers represented by this thesis, it can be tentatively posited that the observed pattern of IFG-putaminal connectivity reflects a human-specific integration of motor/language functions across a vaster portion of this subcortical hub. Indeed, although at surface level a survey of the human neuroimaging literature does not strongly implicate language functions beyond the anterior putamen, fMRI research has shown that speaking in a second or third language of lower than native proficiency activates multiple putaminal regions (Abutalebi et al., 2013) that were demonstrated to have IFG structural connectivity by this research. Abutalebi and colleagues also examined fMRI activation patterns of monolingual speakers but did not find putaminal activity. It could be the case that the left putamen has an anatomical arsenal of motor/language integrative power that is relied on and strengthened when engaged in tasks involving speech articulation in a non-native language. Structural connectivity would become more robust with multilingual experience and exposure due to long-term synaptogenesis, leading to observable anatomical changes that might manifest in research as a function of time or development. Volumetric research appears to support this hypothesis, demonstrating greater grey matter volume of the left putamen for proficient speakers who acquired a second language at birth than for those who learned a second language later on in childhood (Berken, Gracco, Chen, & Klein, 2015). Additionally, significant contrasts between scalar metrics from DWI research comparing monolingual to bilingual speakers have suggested neuroplastic changes in white matter structures potentially containing frontal-putaminal projections, distributed bilaterally although more extensive in the right hemisphere (Singh et al., 2017).

This thesis' streamline networking methodology also enabled native-space, quantitative analyses of the intra-structural topography of cortical networks. Draganski and colleagues (2008) similarly attempted to evaluate network integration/segregation within a probabilistic tractography framework, and produced compelling evidence of subcortical topographical gradients for frontal cortices neighboring the IFG. However, this group used large, multi-gyri ROIs to generate normalized connectivity profiles, differentiating the utility of their methods from this thesis' novel and highly specific application to network relationships. Our topographical analyses were conducted exclusively with thalamic circuits, as a methodological pilot for future exploration with larger, more optimal datasets and additional ROIs.

Cortical circuits from the IFG were primarily segregated intra-thalamically, with some overlap/integration along network boundaries (Figure 12; Table 3). Overlap was greatest for regions shown to co-activate during similar language tasks in fMRI investigations and meta-analyses, specifically POr/PTr for semantic processing and PTr/POp for syntactic functions (reviewed in Sections 2.1 and 2.1.2), suggesting anatomical support for subcortically-integrated, brain-behavior relationships.

Pars orbitalis' (POr) contributions to the language network are not clear. As mentioned, fMRI research has demonstrated that functional changes in both POr and PTr reliably occur for semantic tasks (e.g. Hagoort & Indefry, 2014). Although traditionally only PTr and POp have been associated with syntactic processing, syntax manipulation tasks also variably accompany POr activation (e.g. Cooke et al., 2001). Mounting evidence of POr's subcortical connectivity as well as POr's functional contributions to processing prosody (reviewed in Section 2.1.2) could be central to developing a more comprehensive and cohesive model of this region's significance within the language network. Provided that there are appropriate anatomical substrates linking POr, PTr, and POp to the thalamus and neostriatum, prosody and related behavioral functions might enable POr to participate in or moderate integrative semantic and syntactic processing via support from the subcortical brain. Beyond the scope of this discussion, the underlying functional mechanisms related to prosody might not be language-specific but rather applicable to communication and perception more broadly, considering POr's association with emotional processing (Belyk et al., 2017) and perception of temporal or affective elements of music (Lehne, Rohrmeier, & Koelsch, 2014; Levitin & Menon 2003; Vuust, Roepsdorff, Wallentin, & Østergaard, 2006).

Although intra-thalamic overlap of functionally similar regions arguably provides some evidence for a structural connection between fMRI language research findings and thalamic white matter connectivity, more detailed investigations with methods that permit streamline end-point determination would provide useful insight that is necessary for exploring or validating these claims beyond prospective theory. Unfortunately, to our knowledge it is not currently possible to evaluate neuroanatomy *in vivo* at that level of spatial precision. Similarly, links can be made between the patterns of intra-thalamic white matter segregation demonstrated by this thesis and neuroplastic mechanisms that might contribute to the

positive prognosis for language recovery associated with thalamic aphasia (Graff-Radford & Damasio, 1984; Raymer et al., 1997), however, such theories cannot be substantiated without anatomically informed, multi-modal research with clinical populations. For instance, if it is possible to accurately estimate streamline projections in thalamic stroke patients in spite of consequential imaging obstacles (Budde, Janes, Gold, Turtzo, & Frank, 2011), the presence or robustness of intact circuitry could be correlated with symptomology, behavioral performance, or language recovery. Ideally, the wisdom garnered by conducting structurally-informed, multi-modal research studies designed to explore thalamic aphasia would help cultivate a better understanding of the junction of structural/functional connectivity in the language network and provide insight that could assist with prediction of stroke outcomes. In interim, consideration of intra-thalamic white matter relationships within circumscribed regions (i.e. individual thalamic nuclei) would be more useful for interpretation of thalamic aphasia research given the likelihood of dissociations (Asanuma et al., 1985), thus indicating a future direction of diffusion-based anatomical inquiry directly following from this thesis' research.

Continuing to narrow the gaps between functional and structural neuroimaging with advanced mapping of white matter circuitry is important for addressing inferences drawn from the fMRI literature and for promoting empirically based neurolinguistic theory. All white matter circuits within human behavioral networks need to be described and substantiated, specifically and with replication. This thesis contributes progress towards this goal by replicating, depicting, or quantifying several direct white matter connections of the thalamus, striatum, and IFG in a healthy, young adult sample. Moving forward, diffusion tractography has the potential to further impact scientific understanding of how activation in grey matter structures might affect other structures to influence, enable, or restrict behavior. In particular, strides in MR analysis technology are enabling progressively more informative mapping of complex white matter fiber tracts such as those that project to and from subcortical brain structures. Ultimately, advanced combination of diffusion tractography methods with behavioral data and other *in vivo* imaging modalities can be expected to lead to new and more accurate models of brain-behavior relationships.

REFERENCES

Abutalebi, J., Della Rosa, P. A., Gonzaga, A. K. C., Keim, R., Costa, A., & Perani, D. (2013). The role of the left putamen in multilingual language production. *Brain & Language, 125*(3), 307–315. doi:10.1016/j.bandl.2012.03.009

Alexander, G. E., & Crutcher, M. D. (1990). Functional architecture of basal ganglia circuits: neural substrates of parallel processing. *Trends in Neurosciences*, *13*(7), 266–271. doi:10.1016/0166-2236(90)90107-L

Alexander, G. E., Crutcher, M. D., & Delong, M. R. (1990). Basal ganglia-thalamocortical circuits: Parallel substrates for motor, oculomotor, "prefrontal" and "limbic" functions. *Progress in Brain Research, 85*, 119–146. doi:10.1016/S0079-6123(08)62678-3

Alexander, G. E., DeLong, M. R., & Strick, P. L. (1986). Parallel Organization of Functionally Segregated Circuits Linking Basal Ganglia and Cortex. *Annual Review of Neuroscience*, *9*, 357–381. doi:10.1146/annurev.ne.09.030186.002041

Alexander, M. P., Benson, D. F., & Stuss, D. T. (1989). Frontal lobes and language. *Brain & Language, 37*, 656–691. doi:10.1016/0093-934X(89)90118-1

American Psychiatric Association. (2013). Diagnostic and statistical manual of mental disorders (5th ed.). Washington, DC: Author.

Amunts, K., & Zilles, K. (2015). Architectonic mapping of the human brain beyond Brodmann. *Neuron, 88*(6), 1086–1107. doi:10.1016/j.neuron.2015.12.001

Andersson, J. L. R., Jenkinson, M., & Smith, S. (2007). *Non-linear registration aka spatial normalisation: FMRIB technical report TR07JA2*. *Oxford Centre for Functional Magnetic Resonance Imaging of the Brain, Department of Clinical Neurology, Oxford University, Oxford, UK*. Oxford, United Kingdom.

Andersson, J. L. R., Skare, S., & Ashburner, J. (2003). How to correct susceptibility distortions in spin-echo echo-planar images: Application to diffusion tensor imaging. *NeuroImage*, *20*, 870–888. doi:10.1016/S1053-8119(03)00336-7

Andersson, J. L. R., & Sotiropoulos, S. N. (2016). An integrated approach to correction for off-resonance effects and subject movement in diffusion MR imaging. *NeuroImage*, *125*, 1063–1078. doi:10.1016/j.neuroimage.2015.10.019

Ardila, A. (2010). A proposed reinterpretation and reclassification of aphasic syndromes. *Aphasiology*, *24*(3), 363–394. doi:10.1080/02687030802553704

Arikuni, T., & Kubota, K. (1986). The organization of prefrontocaudate projections and their laminar origin in the macaque monkey: A retrograde study using HRP-gel. *The Journal of Comparative Neurology*, *244*(4), 492–510. doi:10.1002/cne.902440407

Asanuma, C., Andersen, R. A., & Cowan, W. M. (1985). The thalamic relations of the caudal inferior parietal lobule and the lateral prefrontal cortex in monkeys: Divergent cortical projections from cell clusters in the medial pulvinar nucleus. *The Journal of Comparative Neurology*, *241*, 357–81. doi:10.1002/cne.902410309

Assemlal, H. E., Tschumperlé, D., Brun, L., & Siddiqi, K. (2011). Recent advances in diffusion MRI modeling: Angular and radial reconstruction. *Medical Image Analysis*, *15*, 369–396. doi:10.1016/j.media.2011.02.002

Barbas, H., García-Cabezas, M. Á., & Zikopoulos, B. (2013). Frontal-thalamic circuits associated with language. *Brain & Language*, *126*, 49–61. doi:10.1016/j.bandl.2012.10.001

Basser, P. J., Mattiello, J., & LeBihan, D. (1994). Estimation of the effective self-diffusion tensor from the NMR spin echo. *Journal of Magnetic Resonance, Series B*. doi:10.1006/jmrb.1994.1037

Belyk, M., & Brown, S. (2013). Perception of affective and linguistic prosody: An ALE meta-analysis of neuroimaging studies. *Social Cognitive and Affective Neuroscience*, *9*, 1395–1403. doi:10.1093/scan/nst124

Belyk, M., & Brown, S. (2015). Pitch underlies activation of the vocal system during affective vocalization. *Social Cognitive and Affective Neuroscience*, *11*(7), 1078–1088. doi:10.1093/scan/nsv074

Belyk, M., Brown, S., Lim, J., & Kotz, S. A. (2017). Convergence of semantics and emotional expression

within the IFG pars orbitalis. *NeuroImage*, *156*, 240–248. doi:10.1016/j.neuroimage.2017.04.020

Berken, J. A., Gracco, V. L., Chen, J. K., & Klein, D. (2015). The timing of language learning shapes brain structure associated with articulation. *Brain Structure and Function*, *221*(7), 3591–3600. doi:10.1007/s00429-015-1121-9

Bohsali, A. A., Triplett, W., Sudhyadhom, A., Gullett, J. M., McGregor, K., FitzGerald, D. B., … Crosson, B. (2015). Broca's area - Thalamic connectivity. *Brain & Language*, *141*, 80–88. doi:10.1016/j.bandl.2014.12.001

Braaten, A. J., Moore, A. B., Cooley, E. L., & Stringer, A. Y. (2011). Language impairments following basal ganglia stroke: Hold and release functions in cognition. In *Casebook of Clinical Neuropsychology* (pp. 628–641). New York: Oxford University Press.

Broca, P. (1861). Perte de la parole, ramollissement chronique et destruction partielle du lobe antérieur gauche du cerveau. *Bulletins de la Société Anthropologique*, *2*, 235-238.

Broca, P. (1861). Remarques sur le siège de la faculté du langage articulé, suivies d'une observation d'aphémie (perte de la parole). *Bulletins de la Société d'anatomie*, *6*, 330-57.

Broca, P. (1865). Sur le siège de la faculté du langage articulé. *Bulletins de la Société d'Anthropologie de Paris*, *6*, 377-393.

Brunner, R. J., Kornhuber, H. H., Seemüller, E., Suger, G., & Wallesch, C. W. (1982). Basal ganglia participation in language pathology. *Brain & Language*, *16*(2), 281–299. doi:10.1016/0093-934X(82)90087-6

Buchanan, T. W., Lutz, K., Mirzazade, S., Specht, K., Shah, N. J., Zilles, K., & Jäncke, L. (2000). Recognition of emotional prosody and verbal components of spoken language: An fMRI study. *Cognitive Brain Research*, *9*(3), 227–238. doi:10.1016/S0926-6410(99)00060-9

Cancelliere, A. E., & Kertesz, A. (1990). Lesion localization in acquired deficits of emotional expression and comprehension. *Brain and Cognition*, *13*(2), 133–147. doi:10.1016/0278-2626(90)90046-Q

Cheng, H., Wang, Y., Sheng, J., Sporns, O., Kronenberger, W. G., Mathews, V. P., … Saykin, A. J. (2012). Optimization of seed density in DTI tractography for structural networks. *Journal of*

Neuroscience Methods, *203*(1), 264–272. doi:10.1016/j.jneumeth.2011.09.021

Colon-Perez, L. M., Spindler, C., Goicochea, S., Triplett, W., Parekh, M., Montie, E., … Mareci, T. H. (2015). Dimensionless, scale invariant, edge weight metric for the study of complex structural networks. *PLoS ONE*, *10*(7), 1–29. doi:10.1371/journal.pone.0131493

Colon-Perez, L. M., Triplett, W., Bohsali, A., Corti, M., Nguyen, P. T., Patten, C., … Price, C. C. (2015). A majority rule approach for region-of-interest-guided streamline fiber tractography. *Brain Imaging and Behavior*. doi:10.1007/s11682-015-9474-5

Cooke, A., Zurif, E. B., DeVita, C., Alsop, D., Koenig, P., Detre, J., … Grossman, M. (2002). Neural basis for sentence comprehension: Grammatical and short-term memory components. *Human Brain Mapping*, *15*(2), 80–94. doi:10.1002/hbm.10006

Copland, D. A., Chenery, H. J., & Murdoch, B. E. (2000). Persistent deficits in complex language function following dominant nonthalamic subcortical lesions. *Journal of Medical Speech-Language Pathology*, *8*(1), 1–14.

Crosson, B. (1985). Subcortical functions in language: A working model. *Brain & Language*, *25*(2), 257–292. doi:10.1016/0093-934X(85)90085-9

Crosson, B. (1999). Subcortical mechanisms in language: Lexical-semantic mechanisms and the thalamus. *Brain and Cognition*, *40*(2), 414–438. doi:10.1006/brcg.1999.1088

Crosson, B., Garcia, A., McGregor, K., & Wierenga, C. E. (2013). The impact of aging on neural systems for language. In M. F. G. Sandra Koffler, Joel Morgan, Ida Sue Baron (Ed.), *Neuropsychology: Science and practice* (pp. 147–188). New York, NY: Oxford University Press.

Crosson, B., Moberg, P. J., Boone, J. R., Gonzalez Rothi, L. J., & Raymer, A. (1997). Category-specific naming deficit for medical terms after dominant thalamic/capsular hemorrhage. *Brain & Language*, *60*(3), 407–442. doi:10.1006/brln.1997.1899

Crosson, B., Parker, J. C., Kim, A. K., Warren, R. L., Kepes, J. J., & Tully, R. (1986). A case of thalamic aphasia with postmortem verification. *Brain & Language*, *29*(2), 301–314. doi:10.1016/0093-934x(86)90050-7

Damasio, A. R., Damasio, H., Rizzo, M., Varney, N., & Gersch, F. (1982). Aphasia with nonhemorrhagic lesions in the basal ganglia and internal capsule. *Archives of Neurology, 39*(1), 15–20. doi:10.1001/archneur.1982.00510130017003

Damasio, A. R., & Geschwind, N. (1984). The neural basis of language. *Annual Review of Neuroscience, 7*, 127–147. doi:10.1146/annurev.ne.07.030184.001015

De Panfilis, C., & Schwarzbauer, C. (2005). Positive or negative blips? The effect of phase encoding scheme on susceptibility-induced signal losses in EPI. *NeuroImage, 25*, 112–121. doi:10.1016/j.neuroimage.2004.11.014

Desikan, R. S., Ségonne, F., Fischl, B., Quinn, B. T., Dickerson, B. C., Blacker, D., … Killiany, R. J. (2006). An automated labeling system for subdividing the human cerebral cortex on MRI scans into gyral based regions of interest. *NeuroImage, 31*(3), 968–980. doi:10.1016/j.neuroimage.2006.01.021

Devlin, J. T., Matthews, P. M., & Rushworth, M. F. S. (2003). Semantic processing in the left inferior prefrontal cortex: A combined functional magnetic resonance imaging and transcranial magnetic stimulation study. *Journal of Cognitive Neuroscience, 15*(1), 71–84. doi:10.1162/089892903321107837

Dominey, P. F., Inui, T., & Hoen, M. (2009). Neural network processing of natural language: II. Towards a unified model of corticostriatal function in learning sentence comprehension and non-linguistic sequencing. *Brain & Language, 109*, 80–92. doi:10.1016/j.bandl.2008.08.002

Draganski, B., Kherif, F., Klöppel, S., Cook, P. A., Alexander, D. C., Parker, G. J. M., … Frackowiak, R. S. J. (2008). Evidence for segregated and integrative connectivity patterns in the human basal ganglia. *The Journal of Neuroscience, 28*(28), 7143–7152. doi:10.1523/JNEUROSCI.1486-08.2008

Dronkers, N. F., Wilkins, D. P., Van Valin, R. D., Redfern, B. B., & Jaeger, J. J. (2004). Lesion analysis of the brain areas involved in language comprehension. *Cognition, 92*(1–2), 145–177. doi:10.1016/j.cognition.2003.11.002

Fabbro, F., Clarici, A., & Bava, A. (1996). Effects of left basal ganglia lesions on language production. *Perceptual and Motor Skills, 82*(3), 1291–1298. doi:10.2466/pms.1996.82.3c.1291

Fecteau, S., Armony, J. L., Joanette, Y., & Belin, P. (2005). Sensitivity to voice in human prefrontal cortex. *Journal of Neurophysiology*, *94*(3), 2251–2254. doi:10.1152/jn.00329.2005

Fiebach, C. J., Schlesewsky, M., Lohmann, G., Von Cramon, D. Y., & Friederici, A. D. (2005). Revisiting the role of Broca's area in sentence processing: Syntactic integration versus syntactic working memory. *Human Brain Mapping*, *24*(2), 79–91. doi:10.1002/hbm.20070

Fischl, B. (2012). FreeSurfer. *NeuroImage*, *62*(2), 774–781. doi:10.1016/j.neuroimage.2012.01.021

Ford, A. A., Colon-Perez, L., Triplett, W. T., Gullett, J. M., Mareci, T. H., & Fitzgerald, D. B. (2013). Imaging white matter in human brainstem. *Frontiers in Human Neuroscience*, *7*, 1–11. doi:10.3389/fnhum.2013.00400

Ford, A. A., Triplett, W., Sudhyadhom, A., Gullett, J., McGregor, K., Fitzgerald, D. B., … Crosson, B. (2013). Broca's area and its striatal and thalamic connections: A diffusion-MRI tractography study. *Frontiers in Neuroanatomy*, *7*, 1–8. doi:10.3389/fnana.2013.00008

Ford, A., McGregor, K. M., Case, K., Crosson, B., & White, K. D. (2010). Structural connectivity of Broca's area and medial frontal cortex. *NeuroImage*, *52*(4), 1230–7. doi:10.1016/j.neuroimage.2010.05.018

Frühholz, S., & Grandjean, D. (2013). Processing of emotional vocalizations in bilateral inferior frontal cortex. *Neuroscience and Biobehavioral Reviews*, *37*(10), 2847–2855. doi:10.1016/j.neubiorev.2013.10.007

Goldman-Rakic, P. S., & Porrino, L. J. (1985). The primate mediodorsal (MD) nucleus and its projection to the frontal lobe. *The Journal of Comparative Neurology*, *242*(4), 535–560.

Gough, P. M., Nobre, A. C., & Devlin, J. T. (2005). Dissociating linguistic processes in the left inferior frontal cortex with transcranial magnetic stimulation. *The Journal of Neuroscience*, *25*(35), 8010–8016. doi:10.1523/JNEUROSCI.2307-05.2005

Gout, A., Seibel, N., Rouvière, C., Husson, B., Hermans, B., Laporte, N., … Sébire, G. (2005). Aphasia owing to subcortical brain infarcts in childhood. *Journal of Child Neurology*, *20*(12), 1003–1008. doi:http://dx.doi.org/10.1177/08830738050200121401

Greitz, D., Franck, A., & Nordell, B. (1993). On the pulsatile nature of intracranial and spinal CSF-circulation demonstrated by MR imaging. *Acta Radiologica*, *34*(4), 321–328. doi:10.1080/02841859309173251

Haber, S. N., Kunishio, K., Mizobuchi, M., & Lynd-Balta, E. (1995). The orbital and medial prefrontal circuit through the primate basal ganglia. *The Journal of Neuroscience*, *15*(7), 4851–4867.

Hagoort, P. (2005). Broca's complex as the unification space for language. In A. Cutler (Ed.), *Twenty-first Century Psycholinguistics: Four Cornerstones* (pp. 157–172). Mahwah, NJ: Lawrence Erlbaum Associates Publishers.

Hagoort, P., & Indefrey, P. (2014). The neurobiology of language beyond single words. *Annual Review of Neuroscience, 37*, 347–362. doi:10.1146/annurev-neuro-071013-013847

Hillis, A. E., Wityk, R. J., Barker, P. B., Beauchamp, N. J., Gailloud, P., Murphy, K., … Metter, E. J. (2002). Subcortical aphasia and neglect in acute stroke: the role of cortical hypoperfusion. *Brain, 125*, 1094–1104. doi:10.1093/brain/awf113

Hinaut, X., & Dominey, P. F. (2013). Real-time parallel processing of grammatical structure in the fronto-striatal system: A recurrent network simulation study using reservoir computing. *PLoS ONE, 8*(2). doi:10.1371/journal.pone.0052946

Hoy, A. R., Kecskemeti, S. R., & Alexander, A. L. (2015). Free water elimination diffusion tractography: A comparison with conventional and FLAIR DTI acquisitions. *Journal of Magnetic Resonance Imaging, 42*(6), 1572–1581. doi:10.1002/jmri.24925

Hynd, G. W., Hern, K. L., Novey, E. S., Eliopulos, D., Marshall, R., Gonzalez, J. J., & Voeller, K. K. (1993). Attention deficit-hyperactivity disorder and asymmetry of the caudate nucleus. *Journal of Child Neurology, 8*, 339–347. doi:10.1177/088307389300800409

Inase, M., Tokuno, H., Nambu, A., Akazawa, T., & Takado, M. (1999). Corticostriatal and corticosubthalamic input zones from the presupplementary motor area in the macaque monkey: Comparison with the input zones from the supplementary motor area. *Brain Research, 833*(2), 191–201. doi:10.1016/S0006-8993(99)01531-0

Jenkinson, M., Bannister, P., Brady, M., & Smith, S. (2002). Improved optimization for the robust and accurate linear registration and motion correction of brain images. *NeuroImage*, *17*(2), 825–841. doi:10.1006/nimg.2002.1132

Jenkinson, M., & Smith, S. (2001). A global optimisation method for robust affine registration of brain images. *Medical Image Analysis*, *5*(2), 143–156. doi:10.1016/S1361-8415(01)00036-6

Jian, B., & Vemuri, B. C. (2007a). A unified computational framework for deconvolution to reconstruct multiple fibers from diffusion weighted MRI. *IEEE Transactions on Medical Imaging*, *26*(11), 1464–71. doi:10.1109/TMI.2007.907552

Jian, B., & Vemuri, B. C. (2007b). Multi-fiber reconstruction from diffusion MRI using mixture of Wisharts and sparse deconvolution. *Information Processing in Medical Imaging*, *20*, 384–395. doi:10.1007/978-3-540-73273-0_32

Jian, B., Vemuri, B. C., Özarslan, E., Carney, P. R., & Mareci, T. H. (2007). A novel tensor distribution model for the diffusion-weighted MR signal. *NeuroImage*, *37*(1), 164–76. doi:10.1016/j.neuroimage.2007.03.074

Kaas, J. H., & Lyon, D. C. (2007). Pulvinar contributions to the dorsal and ventral streams of visual processing in primates. *Brain Research Reviews*, *55*(2), 285–296. doi:10.1016/j.brainresrev.2007.02.008

Keller, S. S., Crow, T., Foundas, A., Amunts, K., & Roberts, N. (2009). Broca's area: Nomenclature, anatomy, typology and asymmetry. *Brain & Language*, *109*(1), 29–48. doi:10.1016/j.bandl.2008.11.005

Kotz, S. A., Anwander, A., Axer, H., & Knösche, T. R. (2013). Beyond cytoarchitectonics: The internal and external connectivity structure of the caudate nucleus. *PLoS ONE*, *8*(7). doi:10.1371/journal.pone.0070141

Kotz, S. A., Frisch, S., von Cramon, D. Y., & Friederici, A. D. (2003). Syntactic language processing: ERP lesion data on the role of the basal ganglia. *Journal of the International Neuropsychological Society*, *9*(7), 1053–1060. doi:10.1017/S1355617703970093

Lehéricy, S., Ducros, M., Van De Moortele, P. F., Francois, C., Thivard, L., Poupon, C., … Kim, D. S. (2004). Diffusion tensor fiber tracking shows distinct corticostriatal circuits in humans. *Annals of Neurology*, *55*(4), 522–529. doi:10.1002/ana.20030

Lemaire, J. J., Golby, A., Wells, W. M., Pujol, S., Tie, Y., Rigolo, L., … Kikinis, R. (2013). Extended Broca's area in the connectome of language in adults: subcortical single-subject analysis using DTI tractography. *Brain Topography*, *26*(3), 428–441. doi:10.1007/s10548-012-0257-7

Mandelli, M. L., Caverzasi, E., Binney, R. J., Henry, M. L., Lobach, I., Block, N., … Gorno-Tempini, M. L. (2014). Frontal white matter tracts sustaining speech production in primary progressive aphasia. *The Journal of Neuroscience*, *34*(29), 9754–9767. doi:10.1523/JNEUROSCI.3464-13.2014

Martinussen, R. (2015). The overlap of ADHD, reading disorders, and language impairment. *Perspectives on Language and Literacy*, *41*(1), 9–14.

Merrill, J., Sammler, D., Bangert, M., Goldhahn, D., Lohmann, G., Turner, R., & Friederici, A. D. (2012). Perception of words and pitch patterns in song and speech. *Frontiers in Psychology*, *3*, 1–13. doi:10.3389/fpsyg.2012.00076

Middleton, F. A., & Strick, P. L. (2000). Basal ganglia output and cognition: Evidence from anatomical, behavioral, and clinical studies. *Brain and Cognition*, *42*(2), 183–200. doi:10.1006/brcg.1999.1099

Middleton, F. A., & Strick, P. L. (2001). A revised neuroanatomy of frontal-subcortical circuits. In D. G. Lichter & J. L. Cummings (Eds.), *Frontal-subcortical circuits in psychiatric and neurological disorders* (1st ed., pp. 44–58). New York, NY: The Guilford Press.

Milardi, D., Bramanti, P., Milazzo, C., Finocchio, G., Arrigo, A., Santoro, G., … Gaeta, M. (2015). Cortical and subcortical connections of the human claustrum revealed in vivo by constrained spherical deconvolution tractography. *Cerebral Cortex*, *25*, 406–414. doi:10.1093/cercor/bht231

Mills, C. K., & Spiller, W. G. (1907). The symptomatology of lesions of the lenticular zone with some discussion of the pathology of aphasia. *Journal of Nervous & Mental Disease*, *34*(9), 558–588.

Nadeau, S. E., & Crosson, B. (1997). Subcortical aphasia. *Brain & Language*, *58*, 355–402. doi:10.1006/brln.1997.1707

Nambu, A. (2004). A new dynamic model of the cortico-basal ganglia loop. *Progress in Brain Research, 143*, 461–466. doi:10.1016/S0079-6123(03)43043-4

Nambu, A., Tokuno, H., Hamada, I., Kita, H., Imanishi, M., Akazawa, T., … Hasegawa, N. (2000). Excitatory cortical inputs to pallidal neurons via the subthalamic nucleus in the monkey. *Journal of Neurophysiology*, *84*(1), 289–300. doi:10.1016/S0168-0102(98)82646-1

Nishio, Y., Hashimoto, M., Ishii, K., Ito, D., Mugikura, S., Takahashi, S., & Mori, E. (2014). Multiple thalamo-cortical disconnections in anterior thalamic infarction: Implications for thalamic mechanisms of memory and language. *Neuropsychologia*, *53*(1), 264–273. doi:10.1016/j.neuropsychologia.2013.11.025

Ojemann, G. A. (1975). Language and the thalamus: Object naming and recall during and after thalamic stimulation. *Brain and Language*, *2*, 101–120. doi:10.1016/S0093-934X(75)80057-5

Oouchi, H., Yamada, K., Sakai, K., Kizu, O., Kubota, T., Ito, H., & Nishimura, T. (2007). Diffusion anisotropy measurement of brain white matter is affected by voxel size: Underestimation occurs in areas with crossing fibers. *American Journal of Neuroradiology*, *28*(6), 1102–1106. doi:10.3174/ajnr.A0488

Parent, A., & Hazrati, L. N. (1995). Functional anatomy of the basal ganglia. *Brain Research Reviews, 20*, 91–127. doi:10.1016/0165-0173(94)00007-C

Patenaude, B., Smith, S. M., Kennedy, D. N., & Jenkinson, M. (2011). A Bayesian model of shape and appearance for subcortical brain segmentation. *NeuroImage*, *56*(3), 907–922. doi:10.1016/j.neuroimage.2011.02.046

Paulmann, S., Pell, M. D., & Kotz, S. A. (2008). Functional contributions of the basal ganglia to emotional prosody: Evidence from ERPs. *Brain Research*, *1217*, 171–178. doi:10.1016/j.brainres.2008.04.032

Petrides, M., Tomaiuolo, F., Yeterian, E. H., & Pandya, D. N. (2012). The prefrontal cortex: Comparative architectonic organization in the human and the macaque monkey brains. *Cortex*, *48*(1), 46–57. doi:10.1016/j.cortex.2011.07.002

Qiu, A., Crocetti, D., Adler, M., Mahone, E. M., Denckla, M. B., Miller, M. I., & Mostofsky, S. H. (2009). Basal ganglia volume and shape in children with attention deficit hyperactivity disorder. *The American Journal of Psychiatry, 166,* 74–82. doi:10.1176/appi.ajp.2008.08030426

Raymer, A. M., Moberg, P., Crosson, B., Nadeau, S., & Gonzalez Rothi, L. J. (1997). Lexical-semantic deficits in two patients with dominant thalamic infarction. *Neuropsychologia*, *35*(2), 211–219. doi:10.1016/S0028-3932(96)00069-3

Reser, D. H., Richardson, K. E., Montibeller, M. O., Zhao, S., Chan, J. M. H., Soares, J. G. M., … Rosa, M. G. P. (2014). Claustrum projections to prefrontal cortex in the capuchin monkey (Cebus apella). *Frontiers in Systems Neuroscience*, *8*, 1–10. doi:10.3389/fnsys.2014.00123

Rodd, J. M., Vitello, S., Woollams, A. M., & Adank, P. (2015). Localising semantic and syntactic processing in spoken and written language comprehension : An activation likelihood estimation meta-analysis. *Brain & Language, 141*, 89–102. doi:10.1016/j.bandl.2014.11.012

Romanski, L. M., Giguere, M., Bates, J. F., & Goldman-Rakic, P. S. (1997). Topographic organization of medial pulvinar connections with the prefrontal cortex in the rhesus monkey. *The Journal of Comparative Neurology*, *379*(3), 313–332. doi:10.1002/(SICI)1096-9861(19970317)379:3<313::AID-CNE1>3.0.CO;2-6

Sadikot, A. F., & Rymar, V. V. (2009). The primate centromedian-parafascicular complex: Anatomical organization with a note on neuromodulation. *Brain Research Bulletin*, *78*, 122–130. doi:10.1016/j.brainresbull.2008.09.016

Schilman, E. A., Uylings, H. B. M., Galis-de Graaf, Y., Joel, D., & Groenewegen, H. J. (2008). The orbital cortex in rats topographically projects to central parts of the caudate-putamen complex. *Neuroscience Letters*, *432*, 40–45. doi:10.1016/j.neulet.2007.12.024

Selemon, L. D., & Goldman-Rakic, P. S. (1985). Longitudinal topography and interdigitation of corticostriatal projections in the rhesus monkey. *The Journal of Neuroscience*, *5*(3), 776–794.

Sherman, M. S., & Guillery, R. W. (2006). *Exploring the thalamus and its role in cortical function* (2nd ed.). London, England: MIT Press.

Singh, N. C., Rajah, A., Malagi, A., Ramanujan, K., Canini, M., Della Rosa, P. A., … Abutalebi, J. (2017). Microstructural anatomical differences between bilinguals and monolinguals. *Bilingualism: Language and Cognition*, 1–14. doi:10.1017/S1366728917000438

Smith, S. M., Jenkinson, M., Woolrich, M. W., Beckmann, C. F., Behrens, T. E. J., Johansen-Berg, H., … Matthews, P. M. (2004). Advances in functional and structural MR image analysis and implementation as FSL. *NeuroImage*, *23*(Suppl. 1), S208–S219. doi:10.1016/j.neuroimage.2004.07.051

Teichmann, M., Rosso, C., Martini, J. B., Bloch, I., Brugières, P., Duffau, H., … Bachoud-Lévi, A. C. (2015). A cortical-subcortical syntax pathway linking Broca's area and the striatum. *Human Brain Mapping*, *36*, 2270–2283. doi:10.1002/hbm.22769

Turken, A. U., & Dronkers, N. F. (2011). The neural architecture of the language comprehension network: Converging evidence from lesion and connectivity analyses. *Frontiers in Systems Neuroscience*, *5*, 1–20. doi:10.3389/fnsys.2011.00001

Ullman, M. T. (2004). Contributions of memory circuits to language: The declarative/procedural model. *Cognition*, *92*, 231–270. doi:10.1016/j.cognition.2003.10.008

Ullman, M. T. (2006). Is Broca's area part of a basal ganglia thalamocortical circuit? *Cortex*, *42*(4), 981–990.

Ullman, M. T. (2016). The declarative/procedural Model: A neurobiological model of language. In G. Hickok & S. L. Small (Eds.), *Neurobiology of Language* (pp. 953–968). San Diego, CA: Academic Press. doi:10.1016/B978-0-12-407794-2.00076-6

Verstynen, T. D., Badre, D., Jarbo, K., & Schneider, W. (2012). Microstructural organizational patterns in the human corticostriatal system. *Journal of Neurophysiology*, *107*(11), 2984–2995. doi:10.1152/jn.00995.2011

Walker, E. A. (1940). A cytoarchitectural study of the prefrontal area of the macaque monkey. *Journal of Comparative Neurology*, *73*(1), 59–86. doi:10.1002/cne.900730106

Wallesch, C. W. (1985). Two syndromes of aphasia occurring with ischemic lesions involving the basal

ganglia. *Brain & Language*, *25*, 357–361.

Wallesch, C. W. (1997). Symptomatology of subcortical aphasia. *Journal of Neurolinguistics*, *10*(4), 267–275.

Wallesch, C. W., Kornhuber, H. H., Brunner, R. J., Kunz, T., Hollerbach, B., & Suger, G. (1983). Lesions of the basal ganglia, thalamus, and deep white matter: Differential effects on language functions. *Brain & Language*, *20*(2), 286–304. doi:10.1016/0093-934X(83)90046-9

Whitworth, R. H., LeDoux, M. S., & Gould, H. J. (1991). Topographic distribution of connections from the primary motor cortex to the corpus striatum in Aotus trivirgatus. *Journal of Comparative Neurology*, *307*, 177–188. doi:10.1002/cne.903070202

Wildgruber, D., Riecker, A., Hertrich, I., Erb, M., Grodd, W., Ethofer, T., & Ackermann, H. (2005). Identification of emotional intonation evaluated by fMRI. *NeuroImage*, *24*(4), 1233–1241. doi:10.1016/j.neuroimage.2004.10.034

Yushkevich, P. A., Piven, J., Hazlett, H. C., Smith, R. G., Ho, S., Gee, J. C., & Gerig, G. (2006). User-guided 3D active contour segmentation of anatomical structures: Significantly improved efficiency and reliability. *NeuroImage*, *31*(3), 1116–1128. doi:10.1016/j.neuroimage.2006.01.015

APPENDICES

Appendix A: Skull-stripping

All T1-weighted, anatomical images were skull-stripped using FreeSurfer's automated cortical reconstruction battery (Fischl, 2012). Each image was then visually inspected for accuracy to ensure adequate registration in all subsequent steps of processing and analysis.

The FSL-VBM brain extraction module was used for skull-stripping diffusion-weighted images, in consideration of FreeSurfer's considerable computational demands and the distinct requirements of DWI data compared to their accompanying, T1-weighted images. Specifically, the relatively low resolution of $2mm^3$ diffusion-weighted scans and susceptibility artifacts where the frontal sinuses border the orbitofrontal region of the brain pose an added layer of intricacy that requires very intentional skull-stripping in order to analyze DWI data. Thus, conservative skull strips were generated, conflated across multiple trials when necessary, binarized, and manually edited to ensure no data was unintentionally lost.

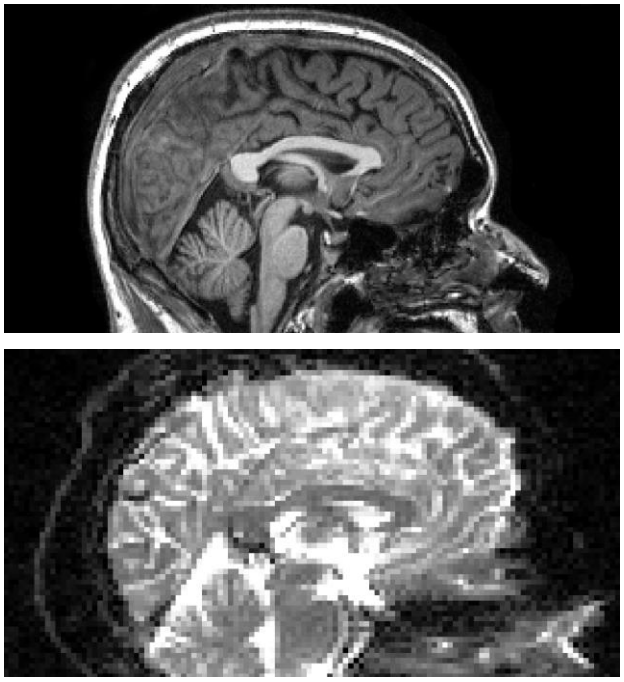

Appendix B: Increasing Surface Area by Dicing ROIs into Component Sub-nodes

Eliminating all streamline vectors that originate from outside an edge (i.e. do not directly connect ROI nodes) increases the specificity and relevance of tractography data and therefore also the validity of quantitative metrics. However, a great deal of data is overlooked if an edge is cropped at the surface of an ROI, as is typical for the purpose of direct structural networking (Colon-Perez, Spindler, et al., 2015). Traceable network streamlines from within deeper layers of an ROI node are missed, in essence inflating the possibility of type II error and ignoring intra-structure streamline trajectories that also represent direct structural connectivity. A relatively simple solution for this conundrum is to strategically increase the surface area of each ROI, without re-conceptualizing the ROI itself, by "dicing" each ROI into the smallest possible unit and iterating network tracking on each of those units as its own network sub-node. The hundreds or thousands of resulting networks can then be combined into a single, panoramic network of edges that comprehensively reflects the full potency of the acquired and reconstructed DWI data.

This solution was actualized by coding a UNIX compatible program, referred to as "PanTrack", which performs these functions from a foundation of binary executables, FSL, AFNI, TrackVis' diffusion toolkit, and the TrackTools software suite developed in Dr. Thomas Mareci's research lab at the University of Florida. Dr. Mareci served as an additional mentor during the development of PanTrack, collaborating with the author to ensure that quantitative metrics were calculated accurately.

The utilized version of PanTrack was coded in Bash to prioritize use of existing software packages and retain elements of prior-validated processing pipelines. As a trade-off, processing time and computational burden was considerable. Additionally, the software relied on for pooling intermediary data was not created for merging within-network files, resulting in unnecessarily large and difficult to manipulate streamline tractography files. Thus, post-processing exclusions were applied only as necessary for interpretation, and neither streamline counts nor track volumes were reported. Please note that these processing limitations will become obsolete in a more efficient computer science framework.

Appendix C: Upsampling Track Files to Increase Data Specificity

Native-space tractography analyses based on volume metrics typically conform to the Cartesian coordinate system and voxel size determined at scan acquisition. In other words, if diffusion-weighted data was acquired with $2mm^3$ voxels, density masks and volume metrics will also be based on $2mm^3$ voxels and compatible with raw or pre-processed images. Maintaining this coordinate system results in a notable loss of specificity when track files are converted into Niftis (or any comparable file format), as track files contain streamline vectors represented at a resolution much finer than $2mm^3$ units. Of relevance, all neural axons that streamlines represent also have diameters considerably smaller than $2mm^3$. For this thesis, linear streamline vectors were launched and traced from 64 evenly-spaced seed points within each $2mm^3$ voxel. Equidistant point coordinates were encoded along 0.25mm intervals at a resolution of over $1nm^3$.

To illustrate the typical conversion from track to Nifti file format in $2mm^3$ native space, a 2D representation of an 8-point sample streamline can be considered.

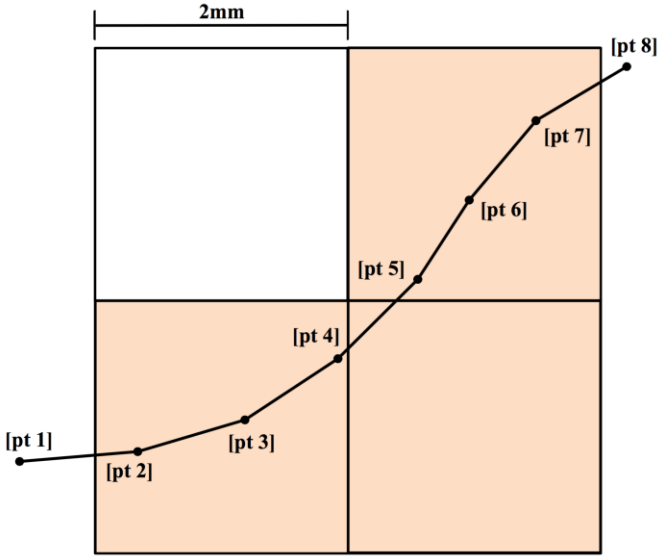

After conversion into a $2mm^2$ grid to create a density mask or calculate "volume", $12mm^2$ of the depicted $16mm^2$ grid would represent this streamline. The shaded boxes represent voxels that would be included in a density mask and used to calculate this numerical value. A great deal of the $12mm^2$ shaded

space coincides with the area surrounding the streamline but not the streamline itself, inevitably resulting in a loss of specificity between file formats.

The format of track files may make it possible to alter the Cartesian coordinate grid used for conversion into Nifti format and/or creating a density mask, without streamline data manipulation. In this context, altering a track file to increase the resolution of the Cartesian coordinate grid used for Nifti conversion will be referred to as "upsampling" a track file. The figure below illustrates the hypothetical result of upsampling the track containing the 8-point sample streamline from $2mm^2$ to $0.5mm^2$ resolution, then converting to Nifti format.

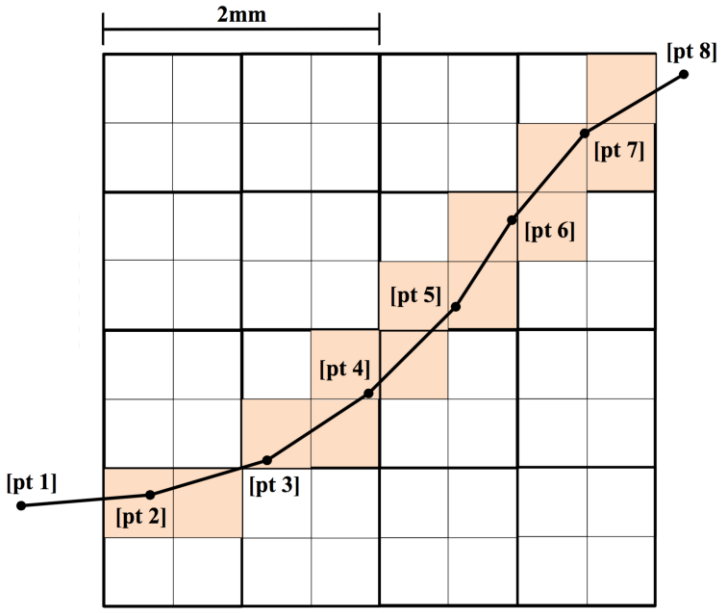

Within the depicted $16mm^2$ pixel grid, only $3.25mm^2$ of space (shaded) represents the 8-point sample streamline. The distance between points along the streamline has not changed, but $8.75mm^2$ of space that does not contain the actual streamline has been eliminated, as compared to the conversion represented by the previous figure. Upsampling the track has fundamentally swapped out the coordinate system the track file has a relationship with for a corresponding but higher resolution coordinate system. Consequently, the result of a file format conversion should have a lesser impact on data specificity.

Further testing is necessary to empirically substantiate methods used to alter track-to-Nifti relationships, and considerations which may arise across streamline tractography reconstruction methods

and parameters must be explored as well. Nonetheless, preliminary data describing intra-thalamic circuit integration/segregation calculated from upsampled tracks was promising. The data from the upsampled tracks reflected the same patterns as those demonstrated by the data reported for this thesis' primary analysis, however the percentage of overlap was substantially less for all groups and visual rendering was more precise (Figure 12; Table 3).

If these preliminary data are in fact based on more specific quantifications of the same white matter networks, there are notable implications for the future of direct, intra-structural networking. The increase in specificity from upsampling may indicate that is it possible to evaluate *in vivo* topography of small, short-range fiber tracts such as those found in the subcortical brain. These implications are particularly promising because track upsampling can be applied to any DWI data acquired with isotropic voxels and does not generate a significant increase in computing burden. By simply re-envisioning the relationship between track files and voxel-based MRI images, it may be possible to increase the specificity and validity of deterministic tractography metrics without sacrificing sensitivity or interpolating the MR signal. More thorough vetting of track file upsampling with larger sample sizes will be necessary to determine if this methodology is truly capable of such feats, but at minimum the possibility merits attention and further inquiry.

Appendix D: *Post-hoc* Analyses

All networks analyzed for this thesis were also processed without the methodological innovations described in Appendix B, for a more direct replication of the research upon which this investigation's methods were based (Bohsali et al., 2015; Ford, Triplett, et al., 2013). Specifically, global tractography data was processed and networked using TrackTools and full ROI masks, without increasing surface area for intra-structural networking or applying post-processing exclusions. This analysis generated no circuits demonstrating direct structural connectivity for POr. Subsequently, it can be inferred that the

methodological innovations used to analyze the data may have made it possible to trace direct POr circuitry as a result of relatively increased sensitivity to cortico-subcortical streamline networks.

For closer comparison of methods and *post-hoc* evaluation of null findings, additional data corresponding to the parameters described by the table below were generated for a single subject (#2) with robust POr/PTr connectivity but null POp findings. Identical streamline exclusions were applied to all cortico-thalamic/thalamo-cortical networks.

Associated Literature	Step Interval	Ang Dev (*ang*)	Seeds/vox (*sd*)	Global Size
a. Primary Analysis (Appendix A)	0.25mm	50°	64	13 GB
b. Primary Analysis – *without innovation**	0.25mm	50°	64	14 GB
c. Ford, Triplett, et al. (2013)	0.25mm	50°	512	103 GB
d. Bohsali et al. (2015)	0.25mm	65°	64	25 GB
e. Bohsali et al. (2015) – *sd modified*	0.25mm	65°	512	195 GB

** Processed with TrackTools instead of PanTrack*

Angular deviation (*ang*) was manipulated to mimic previous research demonstrating pathways between classical Broca's area and segmented thalamic nuclei (Bohsali et al., 2015). Seed density (*sd*) was manipulated to mimic the cumulative seeds/mm of prior research interpolated to $1mm^3$ for processing (Ford, Triplett, et al., 2013). Increases of within-voxel seed density typically result in generating a greater number of streamlines. However, seed density must be optimized to avoid generating spurious streamlines, and increases in seed density can dramatically escalate the required computational and storage demands of tractography (Cheng et al., 2012; Colon-Perez, Spindler, et al., 2015). Indeed, increasing seed density resulted in much larger global tractography file sizes, as did manipulating angular deviation, although to a lesser degree.

Tractography data from the PTr network is depicted on the following page for each set of parameters. It was not possible to render all streamlines due to graphical computing limitations, so it is likely that these images under-represent the robustness of certain tracks (a, d, e). Nonetheless, this data suggests that intra-structural networking represented the data most comprehensively, that using a more

liberal angular deviation parameter would not have increased data integrity, and that a higher seed density might have increased data robustness. However, seed density manipulation was unable to catalyze network tracing success if findings were null for any other set of processing parameters. In other words, although PTr networks could be traced with all methods, only Method (a) succeeded at tracing POr circuits, and no method was successful at tracing POp circuits in this subject.

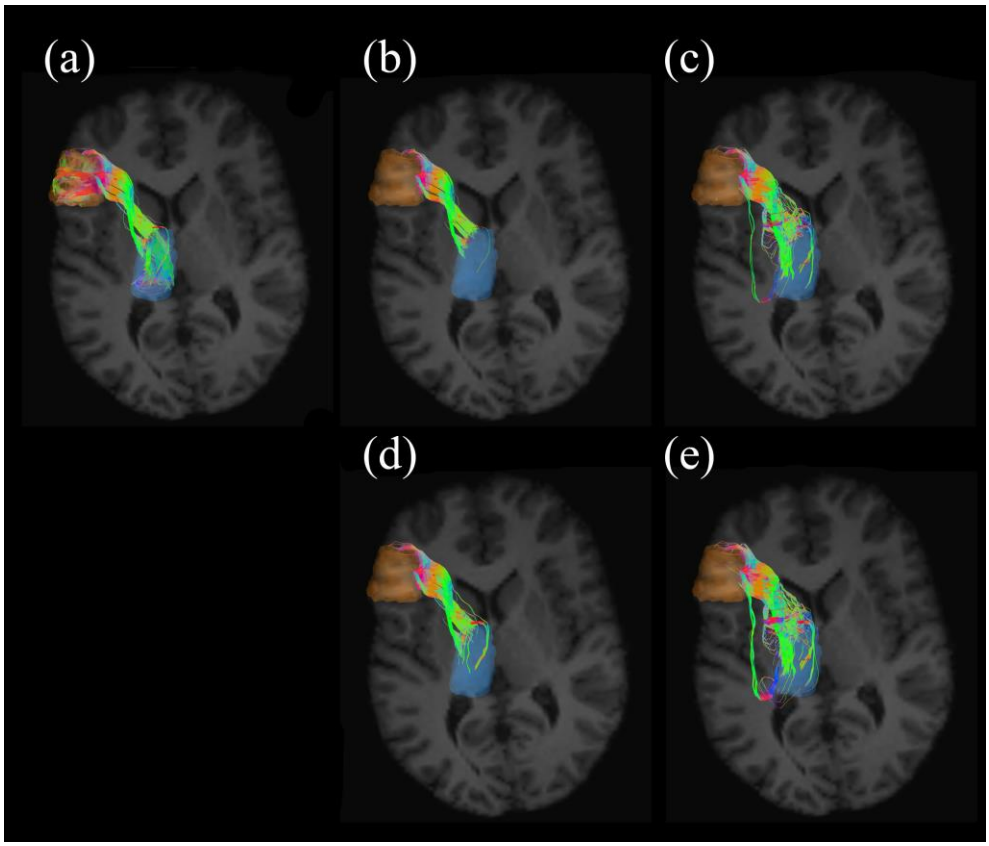

Pars triangularis cortico-thalamic/thalamo-cortical networks: (a) *sd* = 64, *ang* = 50, 25% of streamlines rendered (b) *sd* = 64, *ang* = 50, 100% of streamlines rendered; (c) *sd* = 64, *ang* = 65, 100% of streamlines rendered (d) *sd* = 512, *ang* = 50, 50% of streamlines rendered; (e) *sd* = 512, *ang* = 65, 50% of streamlines rendered

Cortico-thalamic/thalamo-cortical tractography of classical Broca's area was fully processed with Method (b) in one additional subject (#9) for further comparison. Tractography results from this analysis are depicted on the following page. For these images, the streamline rendering settings were comparable and the differing sensitivities of Method (a) and Method (b) are more readily apparent. Both methods

appear to represent qualitatively equivalent networks between Broca's area and the thalamus, however Method (a) produced more robust circuitry and illustrates cortico-thalamic/thalamo-cortical structural connectivity that traverses the length of the thalamus, occupying space in both the ventral anterior and the pulvinar nuclei.

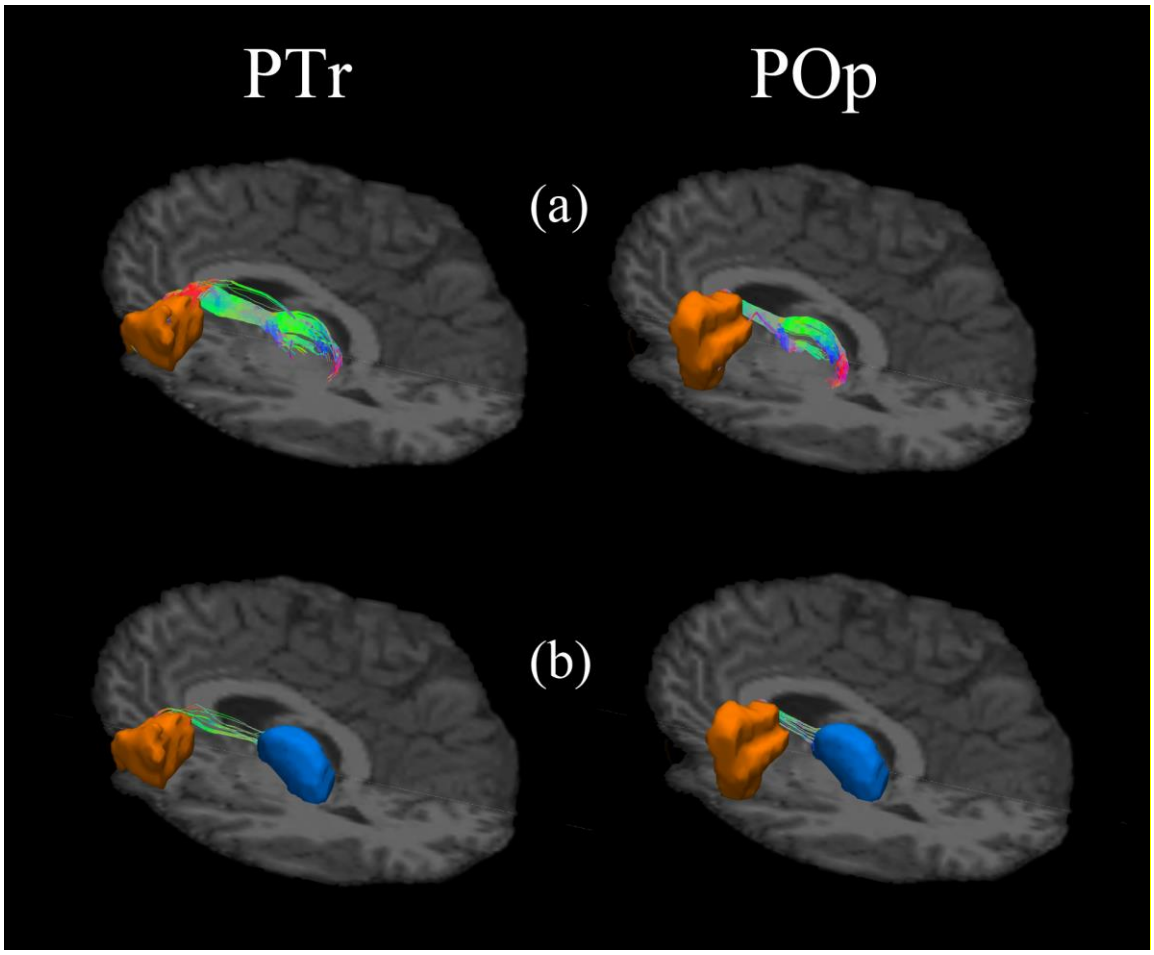

Comparison of Method (a) and Method (b), with cortico-thalamic/thalamo-cortical networks of pars triangularis (PTr) and pars opercularis (POp). The thalamus ROI (blue) is depicted in Method (b) images for visual reference. Cortical ROIs (orange) visually obstruct intra-structural circuitry in both Method (a) images.